JOURNAL OF VIROLOGY, June 2008, p. 6039–6044 Vol. 82, No. 12
0022-538X/08/$08.00+0 doi:10.1128/JVI.02753-07
Copyright © 2008, American Society for Microbiology. All Rights Reserved.

Small Intestine CD4$^+$ T Cells Are Profoundly Depleted during Acute Simian-Human Immunodeficiency Virus Infection, Regardless of Viral Pathogenicity$^\nabla$

Yoshinori Fukazawa,[1]† Ariko Miyake,[1,2]† Kentaro Ibuki,[1] Katsuhisa Inaba,[1] Naoki Saito,[1] Makiko Motohara,[1] Reii Horiuchi,[1] Ai Himeno,[1] Kenta Matsuda,[1] Megumi Matsuyama,[1] Hidemi Takahashi,[3] Masanori Hayami,[1] Tatsuhiko Igarashi,[1] and Tomoyuki Miura[1]*

Laboratory of Primate Model, Experimental Research Center for Infectious Diseases, Institute for Virus Research, Kyoto University, 53 Shogoinkawaramachi, Sakyo-ku, Kyoto 606-8507, Japan[1]; Laboratory of Tumor Cell Biology, Department of Medical Genome Sciences, Graduate School of Frontier Sciences, The University of Tokyo, Tokyo 162-8640, Japan[2]; and Department of Microbiology and Immunology, Nippon Medical School, Tokyo 113-8602, Japan[3]

Received 27 December 2007/Accepted 27 March 2008

To analyze the relationship between acute virus-induced injury and the subsequent disease phenotype, we compared the virus replication and CD4$^+$ T-cell profiles for monkeys infected with isogenic highly pathogenic (KS661) and moderately pathogenic (#64) simian-human immunodeficiency viruses (SHIVs). Intrarectal infusion of SHIV-KS661 resulted in rapid, systemic, and massive virus replication, while SHIV-#64 replicated more slowly and reached lower titers. Whereas KS661 systemically depleted CD4$^+$ T cells, #64 caused significant CD4$^+$ T-cell depletion only in the small intestine. We conclude that SHIV, regardless of pathogenicity, can cause injury to the small intestine and leads to CD4$^+$ T-cell depletion in infected animals during acute infection.

The highly pathogenic simian-human immunodeficiency virus (SHIV) SHIV-C2/1-KS661 (KS661), which was derived from SHIV-89.6 (23), replicates to high titers and causes the irreversible depletion of the circulating CD4$^+$ T cells during the acute phase of intravenous infection, followed by AIDS-like disease within 1 year (23). We previously reported that KS661 massively replicates and depletes CD4$^+$ T cells in both peripheral and mucosal lymphoid tissues during the initial 4 weeks postinfection (16). On the other hand, the isogenic SHIV-#64 (#64), which was derived from SHIV-89.6P, is moderately pathogenic. The genomic sequences of the two SHIVs differ by only 0.16%, resulting in a total of six amino acid changes in the products of the *pol*, *env-gp41*, and *rev* genes. The intravenous inoculation of rhesus macaques with #64 induces plasma viral burdens comparable to those induced by KS661 during the acute phase of infection and causes a transient reduction of the circulating CD4$^+$ T lymphocytes (10). After the acute phase, the viral loads decline to undetectable levels and the populations of CD4$^+$ T cells recover to preinfection levels.

To clarify the relationship between acute viral replication kinetics and subsequent clinical courses for these isogenic SHIVs with distinct pathogenicities, we examined proviral DNA, infectious-virus-producing cells (IVPCs), and CD4$^+$ T-cell depletion in peripheral and mucosal lymphoid tissues of 17 infected (Table 1) and 7 uninfected adult rhesus macaques (*Macaca mulatta*). Both Chinese and Indian rhesus monkeys were randomly assigned to these groups. The monkeys were used in accordance with the institutional regulations approved by the Committee for Experimental Use of Nonhuman Primates of the Institute for Virus Research, Kyoto University, Kyoto, Japan. The animals were inoculated via intrarectal infusion as described previously (17). Following serial euthanasia, tissues were collected and analyzed up to 27 days postinfection (dpi) as described previously (16, 17).

Gross virus replication was assessed by measuring plasma viral loads by reverse transcriptase PCR (16). By 6 dpi, plasma viral RNA levels became detectable in all the KS661-infected macaques (Fig. 1A) and three of seven #64-infected macaques (animals MM372, MM391, and MM374) (Fig. 1B). Although the plasma viral loads of the two groups at 13 dpi, when the virus loads reached their initial peaks, were not significantly different ($P = 0.1673$), the average load (± the standard deviation) in KS661-infected monkeys ($9.3 \times 10^6 \pm 15.9 \times 10^6$ copies/ml) was about 10 times higher than that in #64-infected monkeys ($6.3 \times 10^7 \pm 11.6 \times 10^7$ copies/ml). These results suggest that KS661 spread faster and reached a somewhat higher titer than did #64 when the viruses were inoculated intrarectally.

Levels of peripheral blood CD4$^+$ T lymphocytes in all the KS661-infected monkeys decreased substantially within 4 weeks (Fig. 1C). On the other hand, the reductions in the levels of CD4$^+$ T cells varied among the #64-infected monkeys (Fig. 1D). For example, MM378 did not exhibit any appreciable changes, even though the plasma viral RNA load in this monkey reached 2.6×10^7 copies/ml by 21 dpi (Fig. 1 B and D).

* Corresponding author. Mailing address: Laboratory of Primate Model, Experimental Research Center for Infectious Diseases, Institute for Virus Research, Kyoto University, 53 Shogoinkawaramachi, Sakyo-ku, Kyoto 606-8507, Japan. Phone: 81-75-751-3984. Fax: 81-75-761-9335. E-mail: tmiura@virus.kyoto-u.ac.jp.
† These authors contributed equally to this work.
$^\nabla$ Published ahead of print on 9 April 2007.

Downloaded from jvi.asm.org at Kyoto University on May 22, 2008

TABLE 1. Experimental schedule for individual monkeys[a]

Virus (inoculum size)	Monkeys examined at:		
	6 dpi	13 dpi	27 dpi
KS661 (2×10^3 $TCID_{50}$)	MM300, MM309	MM313, MM334, MM392, MM393	MM308, MM310, MM394, MM395
#64 (2×10^5 $TCID_{50}$)	MM379, MM390	MM372, MM373*, MM391	MM374, MM378

[a] $TCID_{50}$, 50% tissue culture infective doses; *, MM373 received 2×10^3 $TCID_{50}$ of #64.

These data suggest that the decline in circulating $CD4^+$ T cells in KS661-infected animals was more severe and more reproducible than that in the #64-infected monkeys.

Another highly pathogenic SHIV, SHIV-DH12R, is known to cause systemic and synchronous replication events in animals following intravenous inoculation (6). To reveal the spread of virus in monkeys following intrarectal infection, we measured proviral DNA loads in a variety of tissues as described previously (16). KS661 proviral DNA was detected not only in samples from the rectums, the site of virus inoculation, but also in peripheral blood mononuclear cells and some lymph nodes (LN) at 6 dpi (Fig. 2A), suggesting that the virus was already spreading systemically. At 13 dpi, when the viral RNA loads in peripheral blood increased to the highest titers, proviral DNA levels in all of the tissues examined also increased, with levels in most monkeys exceeding 10^4 copies/μg of DNA. The levels of proviral DNA in all the tissues declined remarkably by 27 dpi. In contrast, #64 proviral DNA was detected only in the rectum of one (MM390) of the two monkeys examined at 6 dpi (Fig. 2A). At 13 dpi, the amount of proviral DNA in each tissue sample from #64-infected monkeys ($<10^4$ copies/μg of DNA) was considerably smaller than

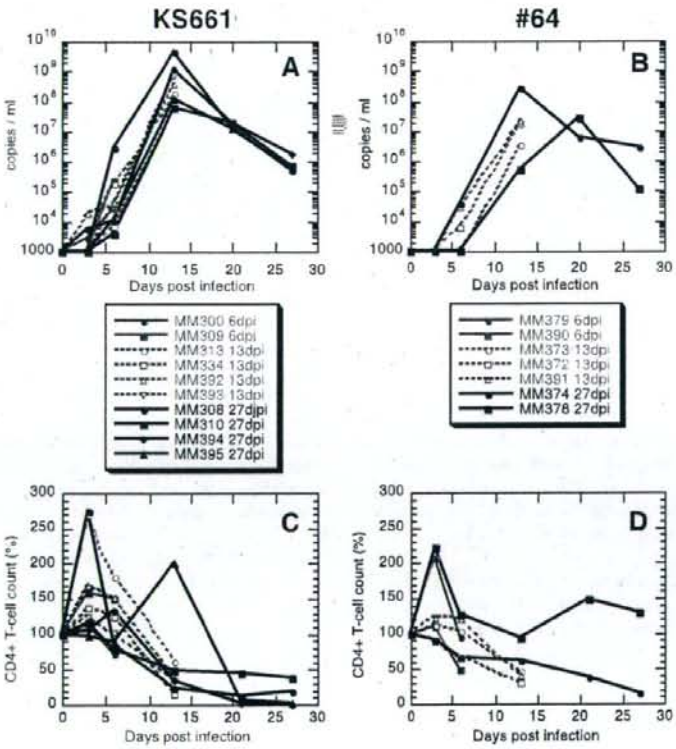

FIG. 1. Plasma viral RNA loads and profiles of circulating $CD4^+$ T cells for monkeys intrarectally infected with highly pathogenic KS661 and moderately pathogenic #64. (A and B) Plasma viral RNA loads were measured by quantitative reverse transcriptase PCR. The detection limit of this assay was 10^3 copies/ml. (C and D) Levels of $CD4^+$ T cells in peripheral blood samples from monkeys infected with KS661 and #64. The absolute number of $CD3^+$ $CD4^+$ cells in peripheral blood immediately before infection (day 0 postinfection) was defined as 100% for each monkey.

Downloaded from jvi.asm.org at Kyoto University on May 22, 2008

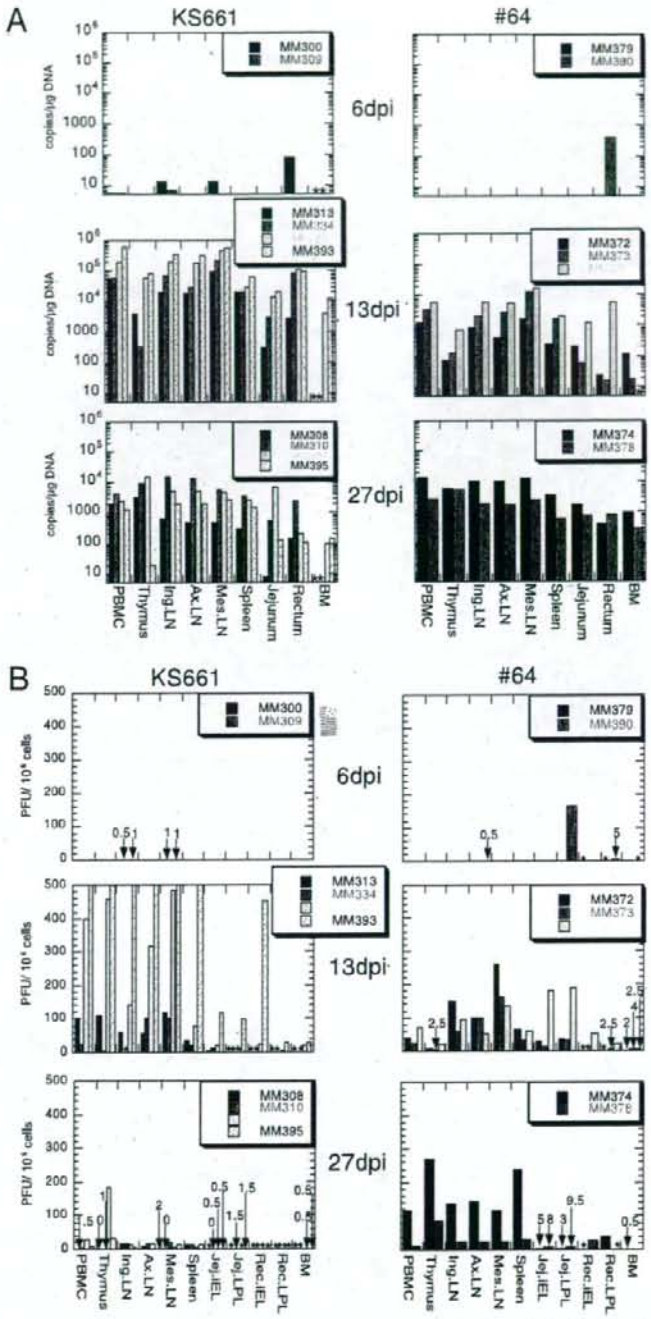

FIG. 2. (A) Proviral DNA loads in tissues of KS661- and #64-infected monkeys at 6, 13, and 27 dpi. Viral burdens were determined by quantitative PCR and expressed as the numbers of viral DNA copies per microgram of total DNA extracted from tissue homogenates. PBMC, peripheral blood mononuclear cells; Ing., inguinal; Ax., axillary; Mes., mesenteric; BM, bone marrow; *, not done. (B) Numbers of IVPCs in tissues of KS661- and #64-infected monkeys at 6, 13, and 27 dpi. Numbers of IVPCs were determined by an infectious plaque assay and were expressed as the numbers of PFU per 10^6 cells. Jej., jejunum; Rec., rectum; iEL, intraepithelial lymphocytes; *, not done.

Downloaded from jvi.asm.org at Kyoto University on May 22, 2008

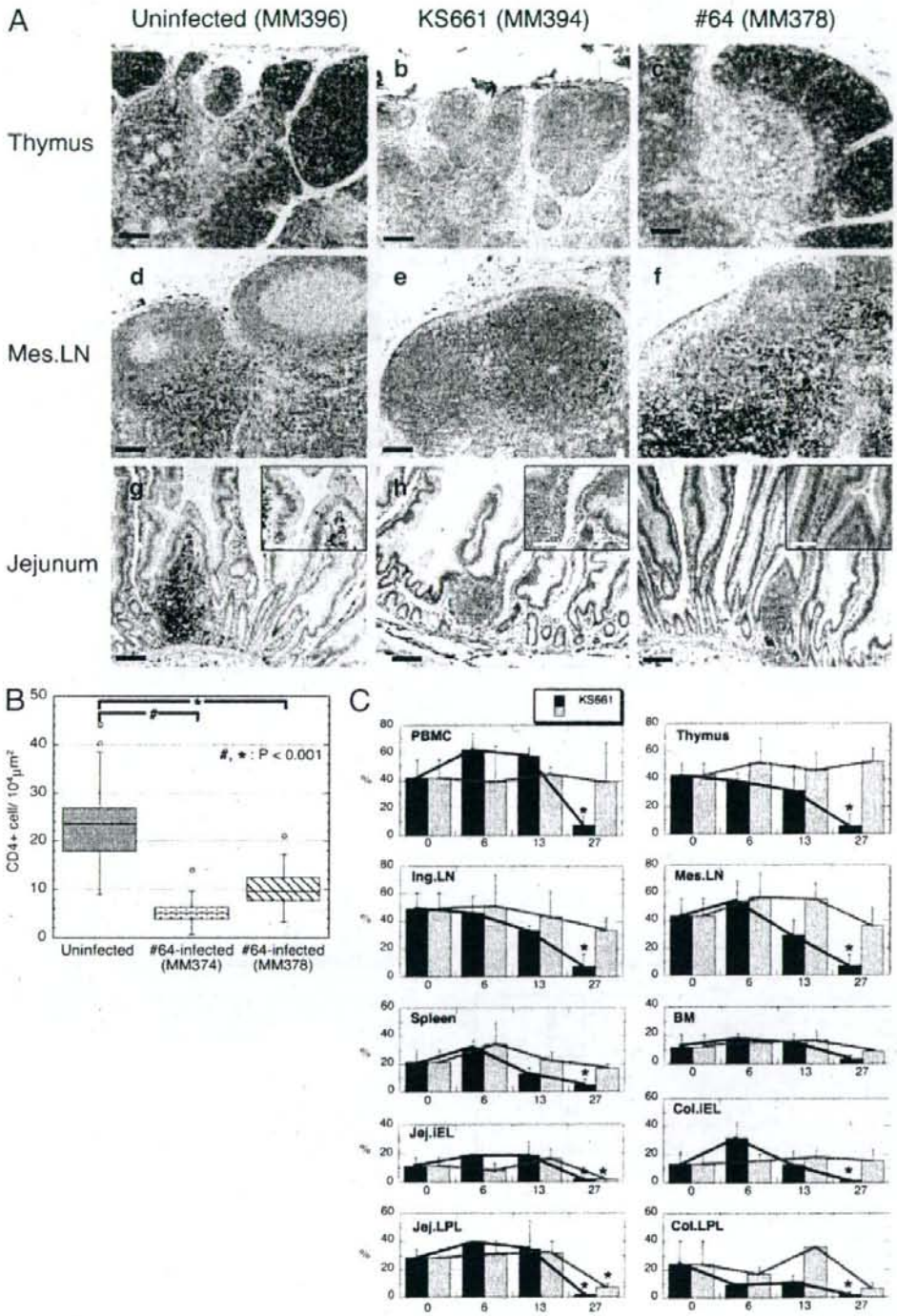

Downloaded from jvi.asm.org at Kyoto University on May 22, 2008

that in each sample from the KS661-infected monkeys. However, unlike the KS661 proviral DNA levels, the #64 proviral DNA levels in most tissues were maintained up to 27 dpi. These results suggest that #64 spread more slowly than KS661 and that the amounts of proviral DNA in a variety of tissues from the #64-infected animals were smaller than those in the tissues from KS661-infected animals around the initial peak of plasma viremia.

Because the amount of proviral DNA measured by PCR may include nonreplicating remnants of the viral genome, we also measured the number of IVPCs in each tissue sample by a plaque assay as described previously (9, 15). Briefly, cells prepared from infected animals were mixed with human T-lymphoid M8166 indicator cells, resuspended in culture medium containing 0.4% agarose, and plated into petri dishes. The plaques that formed in the cell layer were counted after 10 days of cultivation, and the number of IVPCs was calculated. For the KS661-infected monkeys, high numbers of IVPCs in all the tissue samples examined at 13 dpi were detected (Fig. 2B). Among these samples, the thymus and mesenteric LN samples harbored especially high numbers of IVPCs (more than 500/10^6 cells) at 13 dpi. The numbers of IVPCs declined remarkably from 13 to 27 dpi. We concluded that KS661 replicated systemically and synchronously in a variety of tissues, including the intestinal tract, at 13 dpi. In contrast, #64 production patterns in different tissues were not synchronous. Among #64-infected monkeys at 6 dpi, virus production was most active in the jejunum lamina propria lymphocytes (LPL) of MM390 (166 IVPCs/10^6 cells). At 13 dpi, interestingly, mesenteric LN became the center of virus production in two of the three monkeys examined (MM372 and MM373; 259 and 160 IVPCs/10^6 cells). In the other monkey (MM391), the jejunum had the highest number of IVPCs, followed by the mesenteric LN. These results suggested that the virus that replicated in the jejunum spread directly into the mesenteric LN via the flow of lymphatic fluid. At 27 dpi, the thymus tissues of both monkeys examined (MM374 and MM378) exhibited the highest numbers of IVPCs. In summary, the systemic dissemination of #64 was slower than that of KS661, and it was particularly delayed in the thymus during the acute phase.

Systemic $CD4^+$ cell depletion is the signature of disease induced by highly pathogenic SHIVs (7, 8, 22). We therefore compared the frequencies of $CD4^+$ cells in tissues from the animals infected with KS661 and #64, in addition to those of the circulating $CD4^+$ T lymphocytes. As representatives of the major virus-producing organs, the thymus, the mesenteric LN, and the jejunum were selected for examination. CD4 cell numbers were measured by immunohistochemistry analyses as described previously (18). Uninfected thymus tissue contained abundant $CD4^+$ cells that were stained brown (Fig. 3A, panel a), while the tissue collected from the KS661-infected animal at 27 dpi harbored few such cells (Fig. 3A, panel b). #64 caused virtually no $CD4^+$ cell depletion in the thymus at 27 dpi (Fig. 3A, panel c). In the mesenteric LN of uninfected monkeys, $CD4^+$ cells were found in the paracortical region (Fig. 3A, panel d). KS661 depleted $CD4^+$ cells in this area (Fig. 3A, panel e). Unlike KS661, #64 did not reduce the level of $CD4^+$ cells (Fig. 3A, panel f). The jejunum samples from uninfected animals contained $CD4^+$ cells in the lamina propria and follicles of gut-associated lymphatic tissues (Fig. 3 A, panel g). KS661 depleted $CD4^+$ cells in these tissues, too (Fig. 3A, panel h). Interestingly, #64 caused $CD4^+$ cell depletion in the small intestine comparable to that caused by KS661 (Fig. 3A, panel i). To confirm the observed cell reduction in the jejunum samples, we randomly selected a total of 40 fields on the tissue sections from each animal for viewing at a total magnification of ×400, counted $CD4^+$ cells, and averaged the numbers (Fig. 3B). The $CD4^+$ cell densities in the jejunum samples from the #64-infected monkeys were significantly lower than those in the samples from uninfected animals ($P < 0.001$). This gut-specific $CD4^+$ cell depletion caused by #64 prompted us to analyze the frequencies of $CD4^+$ T cells (including CD4 and CD8 doubly positive cells) in a variety of tissues by flow cytometry (Fig. 3C). KS661 caused systemic $CD4^+$ T-lymphocyte depletion by 27 dpi (Fig. 3C). In agreement with the immunohistochemistry results, #64 significantly depleted $CD4^+$ T cells only in the jejunum intraepithelial lymphocytes and LPL ($P = 0.01$ and 0.003, respectively) (Fig. 3C) by 27 dpi, although we examined only two #64-infected monkeys at 27 dpi. In conclusion, the $CD4^+$ T-cell depletion patterns caused by KS661 and #64 were distinct, and the small intestine was the only site in which $CD4^+$ T cells were significantly depleted by the moderately pathogenic #64.

Taken together, our results show that #64 disseminated more slowly and replicated less than KS661 in systemic lymphoid tissues, as well as in peripheral blood, during the acute phase of infection. We believe that because of its low rate and low levels of replication, #64 could not cause irreversible injury before the host mounted an immune reaction. As a result, $CD4^+$ T cells were not completely depleted in all the tissues examined, except in the small intestine. These results suggest that the small intestine is the tissue most sensitive to virus-induced $CD4^+$ T-cell depletion during the acute phase of infection. Recent reports revealed that severe acute depletions

FIG. 3. Profiles of $CD4^+$ T cells in systemic lymphoid tissues during acute infection. (A) Immunohistochemical staining for CD4 molecules (stained brown) in the thymus, mesenteric (mes.) LN, and jejunum tissues of KS661- or #64-infected monkeys at 27 dpi, in addition to those of uninfected monkeys. Black scale bars, 100 μm; white scale bars in insets of panels g, h, and i, 50 μm. (B) Comparison of $CD4^+$ cell frequencies in the jejunum LPL of uninfected and #64-infected monkeys at 27 dpi. A total of forty randomly selected fields (total magnification, ×400) of at least four tissue sections per animal were used for the analysis of jejunum LPL. *P* values (determined by Student's *t* test with 95% confidence intervals) are for comparisons of each #64-infected monkey with uninfected monkeys. (C) Percentages of $CD4^+$ T cells among total lymphocytes from KS661- and #64-infected monkeys. In each graph, data for 0 dpi (time points postinfection are shown along the *x* axis) are averages of percentages for seven uninfected control monkeys. Percentages of $CD4^+$ T cells (including CD4 and CD8 doubly positive cells) were obtained by first gating lymphocytes and then $CD3^+$ T cells with a flow cytometer. PBMC, peripheral blood mononuclear cells; Ing., inguinal; Jej., jejunum; iEL, intraepithelial lymphocytes; BM, bone marrow; Col., colon; *, $P < 0.05$ (percentage at 0 dpi versus that at 27 dpi; Student's *t* test with a 95% confidence interval).

Downloaded from jvi.asm.org at Kyoto University on May 22, 2008

of mucosal CD4$^+$ T cells have been observed in simian immunodeficiency virus-infected monkeys (11, 12, 24, 25) and human immunodeficiency virus-infected humans (2, 5, 13). The acute depletion of mucosal CD4$^+$ T cells and the disease outcome are correlated (1, 3, 21, 26). However, a decrease of mucosal CD4$^+$ T cells has also been observed in the early phases of natural host infections, such as SIVagm infection in African green monkeys and SIVsmm infection in sooty mangabeys, which typically do not progress to AIDS (4, 14, 19). In addition, the levels of apoptosis and immune activation and the degrees of CD4$^+$ T-cell restoration differ between progressors and nonprogressors in simian immunodeficiency virus models (4, 14, 19). Taken together, these results raise the possibility that the severe acute depletion of mucosal CD4$^+$ T cells is not sufficient to induce AIDS. The restoration of CD4$^+$ T cells and normal immune function after the severe acute depletion may define the eventual disease outcome (20). The abilities of KS661- and #64-infected monkeys to restore the immune system may be different, because KS661, but not #64, impairs thymic T-cell differentiation (18). Currently, we are focusing on the restoration of CD4$^+$ T cells and the functional aspect of the immune cells in the small intestines of animals infected with KS661 and #64 to further clarify the determinant(s) of the disease outcome.

We are grateful to James Raymond for English editing of the manuscript and to Takahito Kazama for technical support.

This work was supported, in part, by Research on Human Immunodeficiency Virus/AIDS in Health and Labor Sciences research grants from the Ministry of Health, Labor and Welfare, Japan, a grant-in-aid for scientific research from the Ministry of Education and Science, Japan, a research grant for health sciences focusing on drug innovation for AIDS from the Japan Health Sciences Foundation, and a grant from the Program for the Promotion of Fundamental Studies in Health Sciences of the National Institute of Biomedical Innovation (NIBIO) of Japan.

REFERENCES

1. **Brenchley, J. M., D. A. Price, and D. C. Douek.** 2006. HIV disease: fallout from a mucosal catastrophe? Nat. Immunol. **7**:235–239.
2. **Brenchley, J. M., T. W. Schacker, L. E. Ruff, D. A. Price, J. H. Taylor, G. J. Beilman, P. L. Nguyen, A. Khoruts, M. Larson, A. T. Haase, and D. C. Douek.** 2004. CD4$^+$ T cell depletion during all stages of HIV disease occurs predominantly in the gastrointestinal tract. J. Exp. Med. **200**:749–759.
3. **Chase, A., Y. Zhou, and R. F. Siliciano.** 2006. HIV-1-induced depletion of CD4$^+$ T cells in the gut: mechanism and therapeutic implications. Trends Pharmacol. Sci. **27**:4–7.
4. **Gordon, S. N., N. R. Klatt, S. E. Bosinger, J. M. Brenchley, J. M. Milush, J. C. Engram, R. M. Dunham, M. Paiardini, S. Klucking, A. Danesh, E. A. Strobert, C. Apetrei, I. V. Pandrea, D. Kelvin, D. C. Douek, S. I. Staprans, D. L. Sodora, and G. Silvestri.** 2007. Severe depletion of mucosal CD4$^+$ T cells in AIDS-free simian immunodeficiency virus-infected sooty mangabeys. J. Immunol. **179**:3026–3034.
5. **Guadalupe, M., E. Reay, S. Sankaran, T. Prindiville, J. Flamm, A. McNeil, and S. Dandekar.** 2003. Severe CD4$^+$ T-cell depletion in gut lymphoid tissue during primary human immunodeficiency virus type 1 infection and substantial delay in restoration following highly active antiretroviral therapy. J. Virol. **77**:11708–11717.
6. **Igarashi, T., C. R. Brown, R. A. Byrum, Y. Nishimura, Y. Endo, R. J. Plishka, C. Buckler, A. Buckler-White, G. Miller, V. M. Hirsch, and M. A. Martin.** 2002. Rapid and irreversible CD4$^+$ T-cell depletion induced by the highly pathogenic simian/human immunodeficiency virus SHIV(DH12R) is systemic and synchronous. J. Virol. **76**:379–391.
7. **Igarashi, T., Y. Endo, G. Englund, R. Sadjadpour, T. Matano, C. Buckler, A. Buckler-White, R. Plishka, T. Theodore, R. Shibata, and M. A. Martin.** 1999. Emergence of a highly pathogenic simian/human immunodeficiency virus in a rhesus macaque treated with anti-CD8 mAb during a primary infection with a nonpathogenic virus. Proc. Natl. Acad. Sci. USA **96**:14049–14054.
8. **Joag, S. V., Z. Li, L. Foresman, E. B. Stephens, L.-J. Zhao, I. Adany, D. M. Pinson, H. M. McClure, and O. Narayan.** 1996. Chimeric simian/human immunodeficiency virus that causes progressive loss of CD4$^+$ T cells and AIDS in pig-tailed macaques. J. Virol. **70**:3189–3197.
9. **Kato, S., Y. Hiraishi, N. Nishimura, T. Sugita, M. Tomihama, and T. Takano.** 1998. A plaque hybridization assay for quantifying and cloning infectious human immunodeficiency virus type 1 virions. J. Virol. Methods **72**:1–7.
10. **Kozyrev, I. L., K. Ibuki, T. Shimada, T. Kuwata, T. Takemura, M. Hayami, and T. Miura.** 2001. Characterization of less pathogenic infectious molecular clones derived from acute-pathogenic SHIV-89.6p stock virus. Virology **282**:6–13.
11. **Li, Q., L. Duan, J. D. Estes, Z. M. Ma, T. Rourke, Y. Wang, C. Reilly, J. Carlis, C. J. Miller, and A. T. Haase.** 2005. Peak SIV replication in resting memory CD4$^+$ T cells depletes gut lamina propria CD4$^+$ T cells. Nature **434**:1148–1152.
12. **Mattapallil, J. J., D. C. Douek, B. Hill, Y. Nishimura, M. Martin, and M. Roederer.** 2005. Massive infection and loss of memory CD4$^+$ T cells in multiple tissues during acute SIV infection. Nature **434**:1093–1097.
13. **Mehandru, S., M. A. Poles, K. Tenner-Racz, A. Horowitz, A. Hurley, C. Hogan, D. Boden, P. Racz, and M. Markowitz.** 2004. Primary HIV-1 infection is associated with preferential depletion of CD4$^+$ T lymphocytes from effector sites in the gastrointestinal tract. J. Exp. Med. **200**:761–770.
14. **Milush, J. M., J. D. Reeves, S. N. Gordon, D. Zhou, A. Muthukumar, D. A. Kosub, E. Chacko, L. D. Giavedoni, C. C. Ibegbu, K. S. Cole, J. L. Miamidian, M. Paiardini, A. P. Barry, S. I. Staprans, G. Silvestri, and D. L. Sodora.** 2007. Virally induced CD4$^+$ T cell depletion is not sufficient to induce AIDS in a natural host. J. Immunol. **179**:3047–3056.
15. **Miyake, A., Y. Enose, S. Ohkura, H. Suzuki, T. Kuwata, T. Shimada, S. Kato, O. Narayan, and M. Hayami.** 2004. The quantity and diversity of infectious viruses in various tissues of SHIV-infected monkeys at the early and AIDS stages. Arch. Virol. **149**:943–955.
16. **Miyake, A., K. Ibuki, Y. Enose, H. Suzuki, R. Horiuchi, M. Motohara, N. Saito, T. Nakasone, M. Honda, T. Watanabe, T. Miura, and M. Hayami.** 2006. Rapid dissemination of a pathogenic simian/human immunodeficiency virus to systemic organs and active replication in lymphoid tissues following intrarectal infection. J. Gen. Virol. **87**:1311–1320.
17. **Miyake, A., K. Ibuki, H. Suzuki, R. Horiuchi, N. Saito, M. Motohara, M. Hayami, and T. Miura.** 2005. Early virological events in various tissues of newborn monkeys after intrarectal infection with pathogenic simian human immunodeficiency virus. J. Med. Primatol. **34**:294–302.
18. **Motohara, M., K. Ibuki, A. Miyake, Y. Fukazawa, K. Inaba, H. Suzuki, K. Masuda, N. Minato, H. Kawamoto, T. Nakasone, M. Honda, M. Hayami, and T. Miura.** 2006. Impaired T-cell differentiation in the thymus at the early stages of acute pathogenic chimeric simian-human immunodeficiency virus (SHIV) infection in contrast to less pathogenic SHIV infection. Microbes Infect. **8**:1539–1549.
19. **Pandrea, I. V., R. Gautam, R. M. Ribeiro, J. M. Brenchley, I. F. Butler, M. Pattison, T. Rasmussen, P. A. Marx, G. Silvestri, A. A. Lackner, A. S. Perelson, D. C. Douek, R. S. Veazey, and C. Apetrei.** 2007. Acute loss of intestinal CD4$^+$ T cells is not predictive of simian immunodeficiency virus virulence. J. Immunol. **179**:3035–3046.
20. **Picker, L. J.** 2006. Immunopathogenesis of AIDS virus infection. Curr. Opin. Immunol. **18**:399–405.
21. **Picker, L. J., and D. I. Watkins.** 2005. HIV pathogenesis: the first cut is the deepest. Nat. Immunol. **6**:430–432.
22. **Reimann, K. A., J. T. Li, R. Veazey, M. Halloran, I. W. Park, G. B. Karlsson, J. Sodroski, and N. L. Letvin.** 1996. A chimeric simian/human immunodeficiency virus expressing a primary patient human immunodeficiency virus type 1 isolate *env* causes an AIDS-like disease after in vivo passage in rhesus monkeys. J. Virol. **70**:6922–6928.
23. **Shinohara, K., K. Sakai, S. Ando, Y. Ami, N. Yoshino, E. Takahashi, K. Someya, Y. Suzaki, T. Nakasone, Y. Sasaki, M. Kaizu, Y. Lu, and M. Honda.** 1999. A highly pathogenic simian/human immunodeficiency virus with genetic changes in cynomolgus monkey. J. Gen. Virol. **80**:1231–1240.
24. **Smit-McBride, Z., J. J. Mattapallil, M. McChesney, D. Ferrick, and S. Dandekar.** 1998. Gastrointestinal T lymphocytes retain high potential for cytokine responses but have severe CD4$^+$ T-cell depletion at all stages of simian immunodeficiency virus infection compared to peripheral lymphocytes. J. Virol. **72**:6646–6656.
25. **Veazey, R. S., M. DeMaria, L. V. Chalifoux, D. E. Shvetz, D. R. Pauley, H. L. Knight, M. Rosenzweig, R. P. Johnson, R. C. Desrosiers, and A. A. Lackner.** 1998. Gastrointestinal tract as a major site of CD4$^+$ T cell depletion and viral replication in SIV infection. Science **280**:427–431.
26. **Veazey, R. S., and A. A. Lackner.** 2004. Getting to the guts of HIV pathogenesis. J. Exp. Med. **200**:697–700.

Downloaded from jvi.asm.org at Kyoto University on May 22, 2008

ELSEVIER

INSTITUT PASTEUR

Microbes and Infection 10 (2008) 531–539

www.elsevier.com/locate/micinf

Original article

Construction and infection of a new simian/human immunodeficiency chimeric virus (SHIV) containing the integrase gene of the human immunodeficiency virus type 1 genome and analysis of its adaptation to monkey cells

Hisashi Akiyama [a,1], Misa Ishimatsu [b], Tomoyuki Miura [a], Masanori Hayami [a], Eiji Ido [b,*]

[a] *Laboratory of Primate Model, Experimental Research Center for Infectious Diseases, Institute for Virus Research, Kyoto University, 53 Shogoin-Kawaracho, Kyoto 606-8507, Japan*

[b] *Laboratory for Viral Replication, Center for Emerging Virus Research, Institute for Virus Research, Kyoto University, 53 Shogoin-Kawaracho, Kyoto 606-8507, Japan*

Received 12 July 2007; accepted 4 February 2008
Available online 8 February 2008

Abstract

Expanding the HIV-1-derived regions in the SHIV genome may help to clarify the viral restriction factors determining the host range. In this study, we constructed a new SHIV having the reverse transcriptase and integrase-encoding regions of HIV-1 in addition to the 3′ half genomic region of HIV-1. This SHIV, termed SHIVrti/3rn, could replicate in a monkey $CD4^+$T cell line, HSC-F, although its replication in monkey PBMCs was very weak. After SHIVrti/3rn was passaged in HSC-F cells for 26 weeks, it gradually began to replicate in monkey PBMCs. This monkey-cell-adapted virus, termed SHIVrti/3rnP, could replicate in rhesus macaques. The whole genome of SHIVrti/3rnP was sequenced and was found to differ from SHIVrti/3rn at eleven positions. We constructed a series of mutants having some or all of these mutations and investigated their replication kinetics. The mutational analysis revealed that all of the mutations, but mainly the mutations in *env*, were responsible for the adaptation in HSC-F cells and were enough to replicate in rhesus PBMCs. Of all the SHIVs reported so far that can infect rhesus monkeys in vivo, SHIVrti/3rnP is the one that is genetically the closest to HIV-1.
© 2008 Elsevier Masson SAS. All rights reserved.

Keywords: SHIV; Chimeric virus; Integrase; Animal model; Monkey; Adaptation

1. Introduction

An obstacle to research on human immunodeficiency virus type 1 (HIV-1) is that the only susceptible animal to HIV-1 infection is chimpanzee (*Pan troglodytes*), which is an endangered species. Thus, infection of simian immunodeficiency virus (SIV) in macaque monkeys has been used as an alternative animal model for HIV-1 infection in humans. However, differences between HIV-1 and SIV have limited the utility of SIV/monkey models to test the functions of HIV-1 gene products in vivo. To overcome this limitation, simian/human immunodeficiency chimeric viruses (SHIVs) containing *env* and its adjacent accessory genes of HIV-1 have been constructed and shown to infect monkeys [1,2]. Because SHIVs have the Env proteins of HIV-1, they could be used as challenge viruses to evaluate vaccines targeting Env in monkeys [3]. The prototype SHIVs were non-pathogenic, but other groups developed pathogenic SHIVs by passaging initially avirulent strains of SHIVs in animals [4,5]. These pathogenic SHIVs have proved to be powerful tools for investigating the pathogenic nature of HIV-1. Nowadays, SHIV/monkey systems are widely

* Corresponding author. Tel./fax: +81 75 751 4037.
E-mail address: eido@virus.kyoto-u.ac.jp (E. Ido).
[1] Present address: Department of Virology, University of Heidelberg, Heidelberg, Germany.

1286-4579/$ - see front matter © 2008 Elsevier Masson SAS. All rights reserved.
doi:10.1016/j.micinf.2008.02.001

used to understand the biological properties of HIV-1 and to develop preventive measures against AIDS.

SHIVs have not only helped to establish animal models for HIV-1 infection in humans, but they also have provided important clues about why HIV-1 cannot replicate in monkey cells. The ability of SHIVs to replicate in monkey cells suggested that replaceable genes were not the determinants for the replication defect of HIV-1 in monkey cells. In this respect, *rt*, *vpr*, *vpu*, *tat*, *rev*, *env* and *nef* seemed not to be involved in the species-specific tropism of HIV-1 replication [6]. In addition, the capsid of HIV-1 has been reported to be one of the targets of a restriction factor in monkey cells [7], and a cellular protein TRIM5α was shown to block HIV-1 infection in Old World monkey cells [8]. In other studies, Vif was reported to overcome another species-specific intracellular restriction factor in primate cells [9], and APOBEC3 family proteins as host cell factors were found to be deeply involved in the function of Vif [10]. Besides, a novel restriction factor was identified as Lv2 and the determinants for Lv2 were mapped to *gag* and *env* [11]. Thus, unknown restriction mechanisms may still exist in primate cells.

Our strategy has been to construct SHIVs by expanding the HIV-1-derived regions in the SHIV genome, which may help to clarify the viral restriction factors determining the host range and to elucidate the mechanisms of innate defense against the HIV-1 infection in monkey cells. It was previously shown that the *rt* region of *pol* of SIV can be replaced by that of HIV-1 [12]. Recently, we constructed a new SHIV termed SHIVrt/3rn, which had the *rt* region of *pol* in addition to the 3′ half of the HIV-1 genome [13]. SHIVrt/3rn could infect and replicate not only in monkey peripheral blood mononuclear cells (PBMCs) but also in macaque monkeys. Among the monkey-infecting SHIVs constructed at that time, SHIVrt/3rn had the broadest region of the HIV-1 genome.

In this study, we report the construction of a new SHIV containing the integrase (IN)-encoding region (*int* region) of *pol* of HIV-1 in addition to *rt* and the 3′ half of the HIV-1 genome on the background of SIVmac. The new SHIV, termed SHIVrti/3rn, could replicate not only in monkey PBMCs but also in rhesus monkeys in vivo after adapting to monkey cells. Having *rt*, *int*, *vpu*, *vpr*, *tat*, *rev*, *env* and *nef* of HIV-1, SHIVrti/3rn is much closer to HIV-1 than any other rhesus monkey-infecting SHIVs. Moreover, we constructed a series of mutants containing some or all of the mutations identified in the monkey-cell-adapted strain of SHIVrti/3rn and investigated the effect of the respective mutations on the viral replication. Recently, two HIV-1 derivatives, termed stHIV-1 [14] and NL-DT5 [15] having only the intact *vif* and CA or a part of it of SIV respectively, were found to replicate in rhesus PBMCs after passaging several times in human and/or monkey cell lines. To the best of our knowledge, however, there is no evidence that these derivatives were able to replicate in rhesus monkeys, although the replication of a derivative virus of NL-DT5 (termed NL-DT5R) in pig-tailed macaques was reported very recently [16]. Therefore, we can still say that SHIVrti/3rn is the closest to HIV-1 among the rhesus monkey-infecting SHIVs reported so far.

2. Materials and methods

2.1. DNA constructs

Infectious molecular clones of HIV-1 (pNL432) [17] and SIVmac (pMA239) [18] were used as parental provirus DNAs. In addition, two infectious molecular clones, pSHIV-rti (Ido et al., ms. in preparation) and pNM-3rn [8] were used. The former plasmid contains *rt* and *int* of HIV-1 on an SIVmac background. Briefly, the junction of *pr* of SIVmac and *rt* of HIV-1 was created as described previously [13] and the junction of *int* of HIV-1 and *vif* of SIVmac was created by inserting the PpuMI – PpuMI fragment (nt 5492 and nt 5370 in pMA239) containing the full *vif* of SIVmac between the two AvrII sites in *int* of HIV-1 (nt 5431 and nt 5661 in pNL432) after blunt-ligation. The latter plasmid possesses *env* and adjacent accessory genes such as *vpr*, *vpu*, *tat*, *rev* and *nef* of HIV-1 on an SIVmac background.

A fragment of pSHIV-rti spanning from SpeI (nt 2026 in pMA239, *gag*) to NspV (nt 6131 in pMA239, *vif*) was inserted into the corresponding position of pNM-3rn. The newly generated full-genome plasmid was termed pSHIVrti/3rn (Fig. 1).

Substitution mutant plasmids of pSHIVrti/3rn were created by site-directed mutagenesis by PCR with appropriately modified primers based upon the sequencing analysis. As for the T-to-C mutation in the primer binding site (PBS), we replaced a fragment of pSHIV-rti/3rn spanning from NarI (nt 1079 in pMA239, PBS) to DraIII (nt 1627 in pMA239, *gag*) with the corresponding region of pSHIV-C2/1 KS661. SHIV-C2/1 KS661 is a molecular clone derived from a pathogenic SHIV-C2/1 strain that has the same T-to-C substitution in the PBS [19].

2.2. Cell cultures

M8166, a $CD4^+$ human T cell line, is a subclone of C8166 cells [20]. HSC-F is a cynomolgus monkey $CD4^+$T cell line from a fetal splenocyte that was immortalized by infection with *Herpesvirus saimiri* subtype C [21]. M8166 cells and HSC-F cells were maintained in RPMI 1640 medium containing 10% heat-inactivated fetal bovine serum (FBS). 293T cells were maintained in Dulbecco's modified Eagle's medium containing 10% FBS. PBMCs from healthy rhesus monkeys (*Macaca mulatta*) were cultured as described previously [8]. For the depletion of $CD8^+$ cells, rhesus PBMCs were treated with mouse anti-human CD8 monoclonal antibody (NU-Ts/c; Nichirei, Japan) and sheep anti-mouse IgG magnetic beads (Dynabeads M-450; Dynal A. S, Oslo, Norway).

2.3. Transfection and infection

To generate infectious virus particles, 5 μg of pSHIVrti/3rn was introduced into 1.5×10^6 M 8166 cells by the DEAE-dextran method [18]. The culture medium was changed every 3 days and the supernatant was filtered (0.45 μm pore size) and stored at −80 °C. Then, virion-associated RT activity was measured as described previously [22]. The supernatant

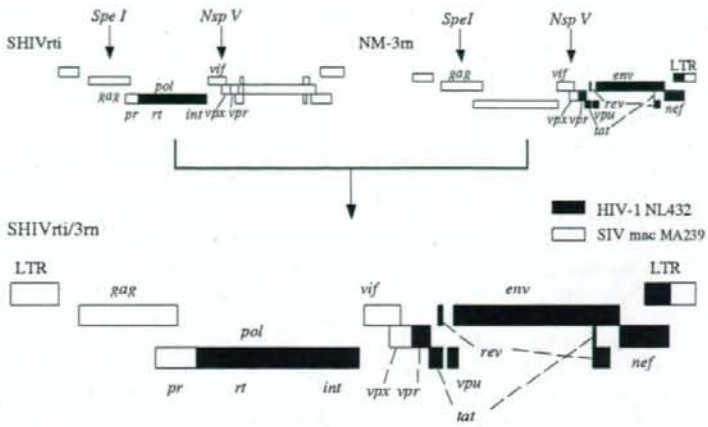

Fig. 1. Genomic structure of a newly constructed SHIVrti/3rn. Solid and open boxes represent sequences derived from HIV-1 (NL432) and SIVmac (MA239), respectively. Arrows indicate the used restriction enzyme sites.

with the highest RT level was used as a virus stock. In the mutational experiment, to avoid unwanted mutations, we transfected 293T cells using FuGene6 (Roche, USA). Twenty-four hours after transfection, we washed the cells once with the medium, and after another 24 h (48 h post transfection) the culture supernatants were harvested, filtered and stored at −80 °C. The virus inoculum used for in vitro infection was adjusted to contain a known amount of RT units (typically 2×10^3 RT units) or multiplicity of infection (moi) by adding the appropriate volume of the medium to the virus stock. M8166 cells (5×10^4 cells/well), HSC-F cells (1×10^5 cells/well) or monkey PBMCs (1×10^5 cells/well) were infected with a virus and cultured in a 96-well plate. The culture supernatant was harvested every 3 days and its RT activity was monitored.

2.4. In vitro passage and inoculum

To adapt SHIVrti/3rn to monkey cells, we passaged the virus in HSC-F cells. Briefly, fresh HSC-F cells were added to SHIVrti/3rn-infected HSC-F cells at a ratio of 1:1 once a week. The culture supernatants were harvested every week. The supernatant of 26 weeks after starting the passage was used for the in vitro and in vivo infection experiments. To determine the viral infectivity of the virus stocks, the 50% tissue culture infectious dose ($TCID_{50}$) was calculated by using M8166 cells or HSC-F cells [6]. The amount of the p27 antigen in the stock was measured with a SIV Core Antigen Assay kit (Coulter, USA).

2.5. DNA sequencing

To identify the nucleotide changes in the SHIVrti/3rn genome that occurred during the passage in monkey cells, we sequenced the viral genome from the beginning of the R region of the 5′ LTR to the end of the U5 region of the 3′ LTR of the passaged SHIVrti/3rn (termed SHIVrti/3rnP). Briefly, total DNA was extracted from the SHIVrti/3rnP-infected HSC-F cells by using a DNeasy Tissue Kit (QIAGEN, Germany). Eight fragments of the viral genome ranging in size from one to two thousand base pairs were then amplified by PCR. The amplified fragments were purified with a QIAquick PCR Purification Kit (QIAGEN, Germany) and sequenced by an automated DNA sequencer (ABI 3100).

2.6. Inoculation of monkeys

All animals were housed in a P3-level monkey storage facility, and were treated in accordance with regulations approved by the Committee for Experimental Use of Non-human Primates in the Institute for Virus Research, Kyoto University. Three adult rhesus monkeys of presumably Chinese origin, MM318 (male), MM319 (female) and MM336 (male), were inoculated intravenously with the virus stock of SHIVrti/3rnP with 2×10^4, 2×10^4 and 1×10^5 $TCID_{50}$, respectively. After the inoculation, blood samples were collected periodically from the monkeys and were separated into plasma and PBMCs. Then, plasma viral RNA loads, proviral DNA, and $CD4^+$T cells and $CD8^+$T cells were analyzed, and virus isolation was attempted by coculturing.

2.7. Detection of proviral DNA in PBMCs

Proviral DNA in PBMCs of inoculated monkeys was detected with nested PCR using the primers designed to specifically amplify the V3 region of HIV-1 (pNL432) *env*, which is present in the SHIVrti/3rn genome, as described previously [13].

2.8. Determination of plasma viral RNA loads

Plasma viral RNA loads were determined by quantitative RT-PCR. The RT reaction and PCR were performed as described previously [23].

2.9. Titration of antibody

Antibody titers of the monkey plasma were measured by particle agglutination according to the instructions of the manufacturer (Genedia HIV-1/2, Fujirebio, Tokyo, Japan).

3. Results

3.1. In vitro replication of SHIVrti/3rn

When M8166 cells were infected with the filtered supernatant that was harvested after transfection with pSHIVrti/3rn, we observed cytopathic effects (CPE) in the infected cells and rising RT activity in the supernatants approximately 2 weeks after infection, indicating pSHIVrti/3rn was capable of producing infectious virions (data not shown).

The replication kinetics of SHIVrti/3rn in M8166 cells, HSC-F cells (a monkey CD4$^+$T cell line) and monkey PBMCs are shown in Fig. 2. In M8166 cells, SHIVrti/3rn started to replicate around 10 days post infection and the virion-associated RT activities gradually increased (Fig. 2a). The replication of SHIVrti/3rn was slower than that of NM-3rn (a parental virus of SHIVrti/3rn) based on their initial rises and peak values. In HSC-F cells, SHIVrti/3rn replicated well, although the replication of SHIVrti/3rn was delayed compared with that of NM-3rn by approximately 9 days and its peak value was somewhat lower (Fig. 2b). In cultured monkey PBMCs, however, the replication of SHIVrti/3rn was very weak and slightly above the detection level, whereas NM-3rn replicated well (Fig. 2c).

3.2. In vitro replication of SHIVrti/3rnP

The RT value of the culture supernatant of HSC-F cells infected with SHIVrti/3rnP reached a peak 9 days after the infection and then gradually decreased (Fig. 2b). Moreover, SHIVrti/3rnP showed a fairly improved replication capacity in rhesus PBMCs compared with the original SHIVrti/3rn (Fig. 2c). On the other hand, the growth-kinetics of SHIVrti/3rnP in M8166 cells was similar to that of the original SHIVrti/3rn (Fig. 2a). These results indicated that SHIVrti/3rnP specifically acquired an ability to replicate in monkey cells including PBMCs.

3.3. In vivo replication of SHIVrti/3rnP

In each of three rhesus monkeys intravenously inoculated with SHIVrti/3rnP, the plasma viral RNA loads reached peak

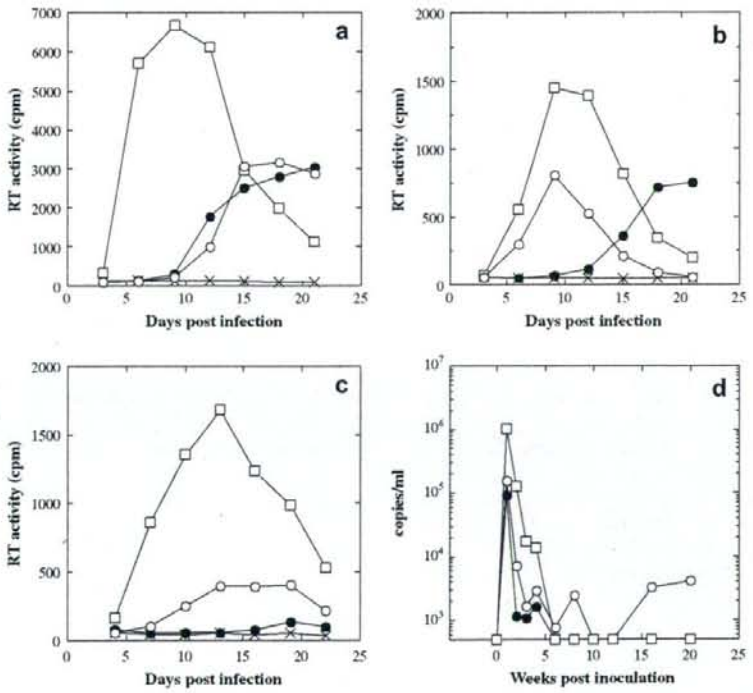

Fig. 2. Growth kinetics of SHIVrti/3rn and SHIVrti/3rnP. Replication of the viruses in (a) a human CD4$^+$T cell line, M8166, (b) a monkey CD4$^+$T cell line, HSC-F, and (c) PBMCs from a rhesus monkey. The cells were infected with SHIVrti/3rnP or cell-free virus stocks from M8166 cells transfected with the respective chimeric DNA clones and virion-associated RT activity in the culture supernatants was monitored. All the experiments were repeated more than three times and representative data are shown. ○, SHIVrti/3rnP; ●, SHIVrti/3rn; □, NM-3rn; ×, mock infection. (d) Plasma viral RNA loads of SHIVrti/3rnP-infected monkeys. Plasma viral RNA loads were measured by quantitative RT-PCR as described in Section 2. ○, MM318; ●, MM319; □, MM336.

Table 1
Virological and immunological statuses of SHIVrti/3rnP-inoculated monkeys

Week	DNA-PCR[a]			Antibody titers[b]		
	MM318	MM319	MM336	MM318	MM319	MM336
0	–	–	–	<32	<32	<32
1	+	+	–	<32	<32	<32
2	+	+	–	1024	512	32
3	+	+	–	2048	1024	64
4	+	+	+	8192	4096	1024
6	+	+	+	8192	4096	1024
8	+	+	+	8192	2048	1024
10	+	+	+	8192	4096	1024
16	+	+	+	8192	≥16,384	4096
20	+	+	+	8192	≥16,384	1024

[a] The presence of viral DNA in PBMCs was determined by PCR using a primer pair for amplification of the V3 region of HIV-1 env. (+) Viral DNA was detected; (–) no viral DNA was detected.
[b] Measured by particle agglutination (Genedia HIV-1/2, Fujirebio).

values (10^4–10^6 copies/ml) at only a week post inoculation (p.i.) (Fig. 2d). The plasma viral RNA loads of MM319 and MM336 gradually decreased and fell below the detectable level at 6 weeks p.i. On the other hand, the plasma viral RNA load of MM318 remained relatively constant and was detectable up to 20 weeks p.i., though it once fell below the detection level at 10 and 12 weeks p.i. Proviral DNAs were continuously detected in PBMCs of all the monkeys from 1 or 3 weeks p.i. to the end of the observation period (Table 1). In all of the monkeys, antibodies were first detected at 2 weeks p.i. and remained at high titers (Table 1). In addition, we reisolated infectious viruses from the PBMCs of one monkey (MM318 at 2 weeks p.i.). These data indicated that SHIVrti/3rnP was competent to infect and replicate in monkeys. On the other hand, none of the monkeys showed any clinical signs or significant changes in the ratio of $CD4^+$ to $CD8^+$T cells, suggesting that SHIVrti/3rnP was non-pathogenic (data not shown).

3.4. Sequence analysis of the passaged viruses

Eleven mutations were found throughout the SHIVrti/3rnP genome, seven of which were within the *env* gene (Table 2). All the substitutions were non-synonymous. The virus obtained from the culture supernatant of the SHIVrti/3rnP-infected PBMCs at around the peak of RT activity was slightly different from SHIVrti/3rnP (Table 2). It differed at the mutation in the matrix region and had two additional mutations, one in the gp120 region and a silent mutation in the gp41 region.

3.5. Construction and in vitro replication of SHIVrti/3rn mutants

Of the 13 mutations (eleven found in SHIVrti/3rnP and two additional in the supernatant of SHIVrti/3rnp-infected rhesus PBMCs), 10 were shared by the two viruses, and therefore were considered more likely to be involved in the adaptation to monkeys. We created five mutants of the original SHIVrti/3rn plasmid, each having a different combination of the 10 mutations (Fig. 3). The plasmids of all the mutants were transfected into 293T cells and the culture supernatants were harvested as virus stocks.

PCAEn and PCAINEn showed almost the same infectivity indices and their values were the highest among all the mutants (Fig. 4a). PCA120 and PCA41 possessed almost the same infectivity indices in HSC-F cells. However, PCA showed a slightly lower infectivity index with this assay system. SHIVrti/3rn hardly replicates in HSC-F cells. Therefore, the value of $TCID_{50}$/ng p27 was much lower than 0.1 and not plottable in Fig. 4a.

In HSC-F cells, PCAEn replicated to the highest titer among the examined constructs (higher than that of SHIVrti/3rnP), and the day of peak was almost the same among

Table 2
Nucleotide mutations in SHIVrti/3rnP

Position[a]		Nucleotide			Amino acid			Genomic region	
nt	Virus	SHIVrti/3rn	SHIVrti/3rnP	rhPBMC[b]	SHIVrti/3rn	SHIVrti/3rnP	rhPBMC[b]		
1085	MA239	T	C	C				PBS	
1316	MA239	T	T/C	T	V	V/A	V	*ma*	
2252	MA239	A	G	G	K	R	R	*ca*	
4245	NL432	G	G/A	G/A	D	D/N	D/N	*int*	
6710	NL432	A	A/G	A/G	S	S/G	S/G		C2
6773	NL432	G	G/A	G/A	D	D/N	D/N	*env*	V2
6803	NL432	A	G	G	N	D	D	(gp120)	C4
7056	NL432	C	T	T	A	V	V		C4
7607	NL432	T	T	T/C	S	S	S/P		V5
7854	NL432	A	G	G	D	G	G		C10
8125	NL432	T	T/A	T/A	N	N/K	N/K	*env*	C11
8350	NL432	T	T	T/C[c]	Y	Y	Y	(gp41)	C12
8463	NL432	A	G	G	N	S	S		C12

[a] Positions in parental pMA239 or pNL432.
[b] Viruses in the supernatant of the SHIVrti/3rnP-infected rhesus PBMCs.
[c] Silent mutation.

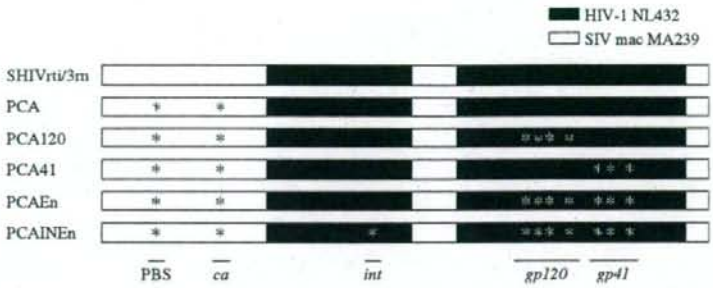

Fig. 3. Genomic structures of newly constructed SHIVrti/3rn mutants. Solid and open boxes represent sequences derived from HIV-1 (NL432) and SIVmac (MA239), respectively. Asterisks indicate the positions of the introduced mutations. PBS, T1085C; ca, A2252G; int, G4245A; gp120, A6710G, G6773A, A6803G and C7056T; gp41, A7854G, T8125A and A8463G.

them (13 days post infection) (Fig. 4b). Thus, it was obvious that PCAEn had the same or better replication capacity than SHIVrti/3rnP, suggesting that the 9 mutations introduced into the PCAEn genome were responsible for the adaptation and both the gp120 and gp41 regions contributed to the adaptation. On the other hand, PCAINEn having all the 10 mutations replicated to a bit lower titer than PCAEn (Fig. 4b), indicating that the additional mutation in *int* appeared to

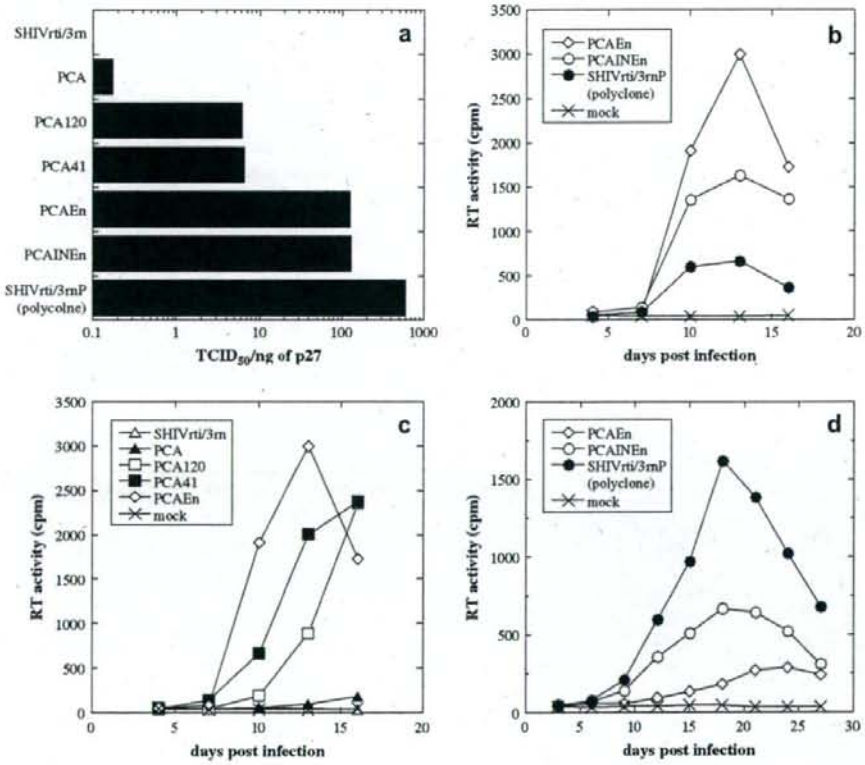

Fig. 4. Biological properties of mutants of SHIVrti/3rn. (a) Infectivity of the mutant viruses. Cell-free virus stock was prepared in 293T by transfection of respective mutated plasmid of SHIVrti/3rn. $TCID_{50}$ was measured in HSC-F cells as described in Materials and methods. Amount of p27 antigen was measured by ELISA and infectivity was defined as $TCID_{50}$ per ng of p27 antigen in this study. (b) and (c), replication kinetics of the mutants in HSC-F cells, and (d) in PBMCs from a rhesus monkey. The cells were infected with the cell-free virus stocks and virion-associated RT activity in the culture supernatants was monitored every 3 days. All the experiments were repeated more than three times and representative data are shown. △, SHIVrti/3rn; ▲, PCA; □, PCA120; ■, PCA41; ◇, PCAEn; ○, PCAINEn; ●, SHIVrti/3rnP (polyclone); ×, mock infection.

have a slightly negative effect on the replication of PCAEn in HSC-F cells. Moreover, PCAEn replicated much faster than SHIVrti/3rn, PCA, PCA120 and PCA41 and the day of peak was around 13 days post infection (Fig. 4c). PCA41 showed almost the same or somewhat better replication capacity than PCA120 in terms of the initial rise of RT activity. These results again indicated that the mutations in both gp120 and gp41 were required for the adaptation. Although PCA showed little infectivity in the $TCID_{50}$ assay (the endpoint was 14 days post infection), it replicated slowly at 15 days post infection. On the other hand, the original SHIVrti/3rn prepared in 293T cells did not show any evidence of replication.

Finally, we inoculated the cells with the mutant viruses at a moi of 0.05 to investigate their replication competence in rhesus PBMCs. To avoid the suppressive effect of $CD8^+$ cells on the viral replication, we employed CD8-depleted PBMCs in this experiment. The polyclonal SHIVrti/3rnP replicated efficiently in the CD8-depleted PBMCs (Fig. 4d). PCAINEn, a putative molecular clone of SHIVrti/3rnP, also replicated well, although the RT value of the day of peak was lower compared to that of SHIVrit/3rnP. On the other hand, the replication competence of PCAEn was fairly weak. Taken together, these results indicate that the mutation in *int* was required for the replication in rhesus PBMCs. Although the replication competence of PCAINEn was not equivalent to that of SHIVrti/3rnP, these results suggested that the 10 mutations in PCAINEn were sufficient to allow it to replicate in rhesus PBMCs and, especially, the mutation in *int* played an important role in the replication competence.

4. Discussion

Since plasma viral RNA loads quickly rose to high titers in monkeys intravenously inoculated with SHIVrti/3rnP (Fig. 2d), SHIVrti/3rnP appears to be suited for use to test whether some antiviral therapies can inhibit the early phase of an HIV-1 infection. Specifically, because SHIVrti/3rnP has RT and IN of HIV-1, it can be used to evaluate the efficacy of therapies that use a combination of HIV-1-specific RT and IN inhibitors. In addition, neutralizing antibodies are generally believed to have a role in preventing HIV-1 infection [24] and passive immunization has been tried in macaques [25]. By using SHIVrti/3rnP having Env of HIV-1, therapies that simultaneously use a combination of replication inhibitors and neutralizing antibodies can be evaluated in vivo. Moreover, because the plasma viral RNA loads of MM318 were maintained up to 20 weeks p.i. (Fig. 2d), SHIVrti/3rnP might infect monkeys persistently. However, in order to use SHIVrti/3rnP to evaluate antiviral therapies during persistent infection, the replication capacity of SHIVrti/3rnP needs to be enhanced and stabilized by further serial animal passages in vivo.

Of the 11 non-synonymous mutations found in SHIVrti/3rnP, seven in *env* were responsible for its adaptation to rhesus monkeys (Fig. 4b). This raises the possibility that the inability of SHIVrti/3rn to replicate in monkey cells involves Env-mediated replication processes such as binding and fusion of incoming virions. Three of the four mutations in the gp120 region were located within the V2 region and its vicinity, a region that was thought not to be involved in receptor and coreceptor binding. The nucleotide at position 7056 (C) in SHIV-NM-3rn, which was substituted with a T in SHIVrti/3rnP (leading to an Alanine-to-Valine substitution), was reported to be associated with the binding of the virion to CD4 [26]. However, because SHIV-NM-3rn replicates well in HSC-F cells, monkey CD4 seems to readily bind to Env of HIV-1. Therefore, it seems unlikely that the change is required in this step to adapt SHIVrti/3rn to monkey cells. As for the mutations in the gp41 region, a G-to-A substitution (nt 7854), which was identified in the SHIVrti/3rnP genome (Table 2), was reported to enhance the fusogenic activity of HIV-1 [27]. Consistent with this observation, cells infected with PCA41, PCAEn and PCAINEn (which have this mutation) showed a more severe CPE than other mutants (data not shown), suggesting that the mutation is involved in the fusion activity. Thus, the enhanced fusion activity of SHIVrti/3rnP might explain its ability to overcome the replication barrier in HSC-F cells. Kamada et al. reported two non-synonymous mutations (nts 6633 and 7043) during the passage of NL-DT5 in a monkey cell line [12]. There were no common mutations between their study and ours.

In this study, we identified several amino acids that appeared to be involved in the adaptation of SHIVrti/3rn to monkey cells. One report argued about the roles of amino acids in the neighboring domains [28]. Nevertheless, the findings in that report are not exactly consistent with the phenomena in this study. For example, the mutation in *ca* is located near the C-terminus of the capsid protein (CA). In HIV-1, the corresponding position of this substitution is located in the hydrophobic core of the crystallographic CA dimer [29]. Mutations in this region resulted in the loss of CA assembly and thus in the loss of infectivity [30]. However, the fact that PCA replicated in HSC-F cells indicated that CA assembly was not severely affected by this mutation. Therefore, the mutations in PBS, *ca* and *int* might be involved in a replication process other than those reported so far. The mutation in CA might be involved in the disassembly of incoming virions. Elucidating the roles of these mutations should uncover new aspects of CA and IN in virus replication.

Preliminary studies in our laboratory indicated that all the mutants constructed in this study show little difference in the processes that occur in the late phase of replication such as production of the viral protein and maturation. Together with the results that mutations in *env* were mainly responsible for the adaptation, we speculate that the adaptation occurred in processes in the early phase of replication such as binding, fusion, and uncoating. At the early stage of HIV-1 infection, a cellular protein, TRIM5α, restricts HIV-1 replication by targeting CA of HIV-1 [7]. Another restriction factor mediated by Gag and Env (known as Lv2) has been reported to work mainly against HIV-2 infection and, in some cases, against HIV-1 infection in monkey cells [11]. Such restrictive mechanisms might also exist in the replication of SHIVrti/3rn in monkey cells.

SHIVrti/3rn has a large HIV-1 component (Fig. 1) and an ability to replicate in monkey PBMCs and in rhesus monkeys

(Figs. 2 and 4 and Table 1). Although two HIV-1 derivatives that has only CA (or a part of it) and the *vif* of SIV were reported to replicate in monkey PBMCs [11,12], there is no evidence that these derivatives were able to replicate in rhesus monkeys. Therefore, we can still say that SHIVrti/3m is the closest to HIV-1 among the rhesus monkey-infecting SHIVs reported so far.

Acknowledgments

We are grateful to Dr. James Raymond for proofreading this manuscript, Dr. Kentaro Ibuki for maintenance of our monkey facility and Takahito Kazama for technical assistance. This work was partly supported by Grant-in-Aid for AIDS Research from the Ministry of Education, Science and Technology and the Ministry of Health, Labor and Welfare of Japan (No. H15-AIDS-002) and Research Grant on Health Sciences focusing on Drug Innovation from the Japan Health Sciences Foundation. H. A. is recipient of a Research Fellowship of the Japanese Foundation for AIDS Prevention and was supported by the 21st Century COE Program of the Ministry of Education, Science and Technology.

References

[1] J. Li, C.I. Lord, C.W. Haseltine, N.L. Letvin, J. Sodroski, Infection of cynomolgus monkeys with a chimeric HIV-1/SIVmac virus that expresses the HIV-1 envelope glycoproteins, J. Acquir. Immune. Defic. Syndr. 5 (7) (1992) 639–646.

[2] S. Sakuragi, R. Shibata, R. Mukai, T. Komatsu, M. Fukasawa, H. Sakai, J. Sakuragi, M. Kawamura, K. Ibuki, M. Hayami, et al., Infection of macaque monkeys with a chimeric human and simian immunodeficiency virus, J. Gen. Virol. 73 (Pt 11) (1992) 2983–2987.

[3] M. Ui, T. Kuwata, T. Igarashi, K. Ibuki, Y. Miyazaki, I.L. Kozyrev, Y. Enose, T. Shimada, H. Uesaka, H. Yamamoto, T. Miura, M. Hayami, Protection of macaques against a SHIV with a homologous HIV-1 Env and a pathogenic SHIV-89.6P with a heterologous Env by vaccination with multiple gene-deleted SHIVs, Virology 265 (2) (1999) 252–263.

[4] S.V. Joag, Z. Li, L. Foresman, E.B. Stephens, L.J. Zhao, I. Adany, D.M. Pinson, H.M. McClure, O. Narayan, Chimeric simian/human immunodeficiency virus that causes progressive loss of $CD4^+$T cells and AIDS in pig-tailed macaques, J. Virol. 70 (5) (1996) 3189–3197.

[5] K.A. Reimann, J.T. Li, R. Veazey, M. Halloran, I.W. Park, G.B. Karlsson, J. Sodroski, N.L. Letvin, A chimeric simian/human immunodeficiency virus expressing a primary patient human immunodeficiency virus type 1 isolate env causes an AIDS-like disease after in vivo passage in rhesus monkeys, J. Virol. 70 (10) (1996) 6922–6928.

[6] T. Kuwata, T. Igarashi, E. Ido, M. Jin, A. Mizuno, J. Chen, M. Hayami, Construction of human immunodeficiency virus 1/simian immunodeficiency virus strain mac chimeric viruses having vpr and/or nef of different parental origins and their in vitro and in vivo replication, J. Gen. Virol. 76 (Pt 9) (1995) 2181–2191.

[7] C.M. Owens, P.C. Yang, H. Gottlinger, J. Sodroski, Human and simian immunodeficiency virus capsid proteins are major viral determinants of early, postentry replication blocks in simian cells, J. Virol. 77 (1) (2003) 726–731.

[8] M. Stremlau, C.M. Owens, M.J. Perron, M. Kiessling, P. Autissier, J. Sodroski, The cytoplasmic body component TRIM5alpha restricts HIV-1 infection in Old World monkeys, Nature 427 (6977) (2004) 848–853.

[9] A.M. Sheehy, N.C. Gaddis, J.D. Choi, M.H. Malim, Isolation of a human gene that inhibits HIV-1 infection and is suppressed by the viral Vif protein, Nature 418 (6898) (2002) 646–650.

[10] M. Malim, Natural resistance to HIV infection: the Vif-APOBEC interaction, C.R. Biol. 329 (11) (2006) 871–875.

[11] C. Schmitz, D. Marchant, S.J. Neil, K. Aubin, S. Reuter, M.T. Dittmar, A. McKnight, Lv2, a novel postentry restriction, is mediated by both capsid and envelope, J. Virol. 78 (4) (2004) 2006–2016.

[12] K. Überla, C. Stahl-Hennig, D. Böttiger, K. Mätz-Rensing, F.J. Kaup, J. Li, W.A. Haseltine, B. Fleckenstein, G. Hunsmann, B. Oberg, et al., Animal model for the therapy of acquired immunodeficiency syndrome with reverse transcriptase inhibitors, Proc. Natl. Acad. Sci. USA 92 (1995) 8210–8214.

[13] H. Akiyama, E. Ido, W. Akahata, T. Kuwata, T. Miura, M. Hayami, Construction and in vivo infection of a new simian/human immunodeficiency virus chimera containing the reverse transcriptase gene and the 3′ half of the genomic region of human immunodeficiency virus type 1, J. Gen. Virol. 84 (Pt 7) (2003) 1663–1669.

[14] T. Hatziioannou, M. Princiotta, M. Piatak Jr., F. Yuan, F. Zhang, J.D. Lifson, P.D. Bieniasz, Generation of simian-tropic HIV-1 by restriction factor evasion, Science 314 (2006) 95.

[15] K. Kamada, T. Igarashi, M.A. Martin, B. Khamsri, K. Hatcho, T. Yamashita, M. Fujita, T. Uchiyama, A. Adachi, Generation of HIV-1 derivatives that productively infect macaque monkey lymphoid cells, Proc. Natl. Acad. Sci. USA 103 (2006) 16959–16964.

[16] T. Igarashi, R. Iyengar, R.A. Byrum, A. Buckler-White, R.L. Dewar, C.E. Buckler, H.C. Lane, K. Kamada, A. Adachi, M.A. Martin, Human immunodeficiency virus type 1 derivative with 7% simian immunodeficiency virus genetic content is able to establish infections in pig-tailed macaques, J. Virol. 81 (20) (2007) 11549–11552.

[17] A. Adachi, H.E. Gendelman, S. Koenig, T. Folks, R. Willey, A. Rabson, M.A. Martin, Production of acquired immunodeficiency syndrome-associated retrovirus in human and non-human cells transfected with an infectious molecular clone, J. Virol. 59 (1986) 284–291.

[18] Y.M. Naidu, H.W. Kestler 3rd, Y. Li, C.V. Butler, D.P. Silva, D.K. Schmidt, C.D. Troup, P.K. Sehgal, P. Sonigo, M.D. Daniel, et al., Characterization of infectious molecular clones of simian immunodeficiency virus (SIVmac) and human immunodeficiency virus type 2: persistent infection of rhesus monkeys with molecularly cloned SIVmac, J. Virol. 62 (1988) 4691–4696.

[19] K. Shinohara, K. Sakai, S. Ando, Y. Arai, N. Yoshino, E. Takahashi, K. Someya, Y. Suzaki, T. Nakasone, Y. Sasaki, M. Kaizu, Y. Lu, M. Honda, A highly pathogenic simian/human immunodeficiency virus with genetic changes in cynomolgus monkey, J. Gen. Virol. 80 (Pt 5) (1999) 1231–1240.

[20] P.R. Clapham, R.A. Weiss, A.G. Dalgleish, M. Exley, D. Whitby, N. Hogg, Human immunodeficiency virus infection of monocytic and T-lymphocytic cells: receptor modulation and differentiation induced by phorbol ester, Virology 158 (1987) 44–51.

[21] H. Akari, K. Mori, K. Terao, I. Otani, M. Fukasawa, R. Mukai, Y. Yoshikawa, In vitro immortalization of Old World monkey T lymphocytes with Herpesvirus saimiri: its susceptibility to infection with simian immunodeficiency viruses, Virology 218 (1996) 382–388.

[22] R.L. Willey, D.H. Smith, L.A. Lasky, T.S. Theodore, P.L. Earl, B. Moss, D.J. Capon, M.A. Martin, In vitro mutagenesis identifies a region within the envelope gene of the human immunodeficiency virus that is critical for infectivity, J. Virol. 62 (1988) 139–147.

[23] I.L. Kozyrev, T. Miura, T. Takemura, T. Kuwata, M. Ui, K. Ibuki, T. Iida, M. Hayami, Co-expression of interleukin-5 influences replication of simian/human immunodeficiency viruses in vivo, J. Gen. Virol. 83 (2002) 1183–1188.

[24] D.R. Burton, Antibodies, viruses and vaccines, Nat. Rev. Immunol. 2 (9) (2002) 706–713.

[25] R.M. Ruprecht, F. Ferrantelli, M. Kitabwalla, W. Xu, H.M. McClure, Antibody protection: passive immunization of neonates against oral AIDS virus challenge, Vaccine 21 (24) (2003) 3370–3373.

[26] P.D. Kwong, R. Wyatt, J. Robinson, R.W. Sweet, J. Sodroski, W.A. Hendrickson, Structure of an HIV gp120 envelope glycoprotein

in complex with the CD4 receptor and a neutralizing human antibody, Nature 393 (6686) (1998) 648–659.
[27] M. Kinomoto, M. Yokoyama, H. Sato, A. Kojima, T. Kurata, K. Ikuta, T. Sata, K. Tokunaga, Amino acid 36 in the human immunodeficiency virus type 1 gp41 ectodomain controls fusogenic activity: implications for the molecular mechanism of viral escape from a fusion inhibitor, J. Virol. 79 (10) (2005) 5996–6004.
[28] K. Soderberg, L. Denekamp, S. Nikiforow, K. Sautter, R.C. Desrosiers, L. Alexander, A nucleotide substitution in the tRNA(Lys) primer binding site dramatically increases replication of recombinant simian immunodeficiency virus containing a human immunodeficiency virus type 1 reverse transcriptase, J. Virol. 76 (11) (2002) 5803–5806.
[29] J. Lanman, T.T. Lam, S. Barnes, M. Sakalian, M.R. Emmett, A.G. Marshall, P.E. Prevelige Jr., Identification of novel interactions in HIV-1 capsid protein assembly by high-resolution mass spectrometry, J. Mol. Biol. 325 (4) (2003) 759–772.
[30] B.K. Ganser-Pornillos, U.K. von Schwedler, K.M. Stray, C. Aiken, W.I. Sundquist, Assembly properties of the human immunodeficiency virus type 1 CA protein, J. Virol. 78 (5) (2004) 2545–2552.

Biochemical and Biophysical Research Communications 377 (2008) 889–893

Contents lists available at ScienceDirect

Biochemical and Biophysical Research Communications

journal homepage: www.elsevier.com/locate/ybbrc

Trans-species activation of human T cells by rhesus macaque CD1b molecules

Daisuke Morita [a,b], Kumiko Katoh [a,b], Toshiyuki Harada [c], Yoshiaki Nakagawa [c], Isamu Matsunaga [a,b], Tomoyuki Miura [d], Akio Adachi [e], Tatsuhiko Igarashi [d,*], Masahiko Sugita [a,b,*]

[a] Laboratory of Cell Regulation, Institute for Virus Research, Kyoto University, 53 Kawahara-cho, Shogoin, Sakyo-ku, Kyoto 606-8507, Japan
[b] Laboratory of Cell Regulation and Molecular Network, Graduate School of Biostudies, Kyoto University, Kyoto 606-8501, Japan
[c] Division of Applied Life Sciences, Graduate School of Agriculture, Kyoto University, Kyoto 606-8502, Japan
[d] Laboratory of Primate Model, Institute for Virus Research, Kyoto University, Kyoto 606-8507, Japan
[e] Department of Virology, Institute of Health Biosciences, The University of Tokushima Graduate School, Tokushima 770-8503, Japan

ARTICLE INFO

Article history:
Received 11 October 2008
Available online 23 October 2008

Keywords:
Rhesus macaque
CD1
Mycobacteria
Glucose monomycolate

ABSTRACT

Despite crucial importance of non-human primates as a model of human infectious diseases, group 1 CD1 genes and proteins have been poorly characterized in these species. Here, we isolated *CD1A*, *CD1B*, and *CD1C* cDNAs from rhesus macaque lymph nodes that encoded full-length CD1 proteins recognized specifically by monoclonal antibodies to human CD1a, CD1b, and CD1c molecules, respectively. The monkey group 1 CD1 isoforms contained amino acid residues and motifs known to be critical for intramolecular disulfide bond formation, N-linked glycosylation, and endosomal trafficking as in human group 1 CD1 molecules. Notably, monkey CD1b molecules were capable of presenting a mycobacterial glycolipid to human CD1b-restricted T cells, providing direct evidence for their antigen presentation function. This also detects for the first time a trans-species crossreaction mediated by group 1 CD1 molecules. Taken together, these results underscore substantial conservation of the group 1 CD1 system between humans and rhesus macaque monkeys.
© 2008 Elsevier Inc. All rights reserved.

Besides MHC class I- and II-restricted αβ T cells that recognize protein antigens (Ags), discrete subsets of T cells exist in humans that specifically recognize non-protein Ags in a T-cell receptor (TCR)-dependent manner. These include αβ T cells that recognize lipid, glycolipid, and lipopeptide Ags in the context of group 1 CD1 molecules (CD1a, CD1b, and CD1c) as well as Vγ2⁺Vδ2⁺ γδ T cells that recognize pyrophosphorylated isoprenoid intermediates [1,2]. Both T cell subsets have been implicated in host defense against mycobacterial infection [3], and therefore, animal species that have evolved these T cells in addition to MHC-restricted T cells would serve as an ideal animal model of human tuberculosis. The murine model has long been studied extensively, and by taking advantage of versatile genetic manipulation and a fine array of reagents, many important aspects of host defense against tuberculosis have been demonstrated explicitly, that include a critical role for MHC-restricted T cells [4]. However, a significant difference in pathology has been noted between the two species [3], and the lack of T cells in mice that cor respond to human group 1 CD1-resricted T cells and Vγ2⁺Vδ2⁺ γδ T cells makes the animals less useful particularly in an attempt to develop a new chemical class of non-protein vaccines against tuberculosis. In contrast to mice and rats, guinea pigs exhibit pathology that is comparable, if not identical, to that in human tuberculosis, and recent studies have shown that they contain four *CD1B* genes and three *CD1C* genes [5,6]. Nevertheless, CD1a-restricted T cells as well as CD1d-restricted NKT cells may not exist in guinea pigs. These and other significant differences in the organization and function of the immune system between humans and rodents often make it difficult to translate the results obtained from rodent models to humans. Further, certain human pathogens, such as HIV-1, exhibit highly limited host selectivity, and are unable to infect into rodents and other commonly used laboratory animals.

Recently, the value of non-human primates as a model of human infectious diseases has been appreciated greatly for elucidating pathogenesis and for developing vaccines and therapies against microbial infections, such as AIDS and tuberculosis [7,8]. Nevertheless, little has been defined about the genes, proteins, and function of the group 1 CD1 molecules in non-human primates, and therefore, the present study was aimed at identifying the rhesus macaque group 1 CD1 system. We found it highly comparable to that in humans, and rhesus macaque CD1b molecules were indeed able to present a human CD1b-presented mycobacterial glycolipid Ag to specific human T cells.

* Corresponding authors. Fax: +81 75 752 3232 (M. Sugita), +81 75 761 9335 (T. Igarashi).
E-mail addresses: tigarash@virus.kyoto-u.ac.jp (T. Igarashi), msugita@virus.kyoto-u.ac.jp (M. Sugita).

0006-291X/$ - see front matter © 2008 Elsevier Inc. All rights reserved.
doi:10.1016/j.bbrc.2008.10.075

Materials and methods

Isolation of rhesus macaque group 1 CD1 cDNAs. Rhesus monkeys (*Macaca mulatta*) were used in accordance with the institutional regulations approved by the Committee for Experimental Use of Nonhuman Primates of the Institute for Virus Research, Kyoto University, Kyoto, Japan. Total RNA was extracted from rhesus macaque lymph nodes using the RNeasy mini kit (Qiagen, Hilden, Germany), and the first-strand cDNA was synthesized from 0.5 mg of the total RNA using oligo(dT) and PrimeScript reverse transcriptase (Takara Bio, Inc., Otsu, Japan). To amplify specific transcripts, the samples were subjected to PCR amplification with *Pfu* DNA polymerase (Stratagene, La Jolla, CA) for 35 cycles of 30 s at 94 °C, 1 min at 55 °C (for *CD1A*) or 60 °C (for *CD1B* and *CD1C*), 2 min at 72 °C, and a final cycle of 10 min at 72 °C. The primers used were: 5′-GCG GTA CCA AAT AAC ATC TGC AAA TGA C-3′ (sense) and 5′-GCC TCG AGA AGG AGG ATC ATG GTG TAT C-3′ (anti-sense) for *CD1A*; 5′-GCG GTA CCA GTA AGA AGT TGC ATC TCC C -3′ (sense) and 5′-GCC TCG AGG GAG CAG ACA TGG TGA GGG C-3′ (anti-sense) for *CD1B*; 5′-GCG GGT ACC ACC ATG CTG TTT CTG CAG TTT-3′ (sense) and 5′-GCG GCG GCC GCA TTG TAC TAG GCT CCT GG-3′ (anti-sense) for *CD1C*. The PCR products were purified and cloned into pcDNA3.1(+) (Invitrogen, Carlsbad, CA), and DNA sequencing was done in both directions. This procedure was repeated twice to confirm that no PCR-associated errors were introduced.

Transfection. A rhesus macaque kidney epithelial cell line, LLC-MK2 [9], was obtained from ATCC (Manassas, VA). The cells were transfected with pcDNA3.1(+) containing either rhesus macaque *CD1A*, *CD1B*, or *CD1C* by a calcium phosphate precipitation method, using the mammalian transfection kit (Stratagene). The transfected cells were then cultured in DMEM media (Invitrogen) supplemented with 10% fetal calf serum (Hyclone, Logan, UT) and G418 (0.5 mg/ml) (Invitrogen), and the CD1-expressing cells were then enriched by labeling with specific antibodies (Abs), followed by positive selection with magnetic beads coated with goat anti-mouse IgG Abs (Invitrogen). A human lymphoblastoid cell line, T2 [10], was transfected with pCEP4 (Invitrogen) containing *CD1A* or *CD1B* of either human or rhesus macaque origin by electroporation as described [11], followed by selection in RPMI1640 media (Invitrogen) containing 0.2 mg/ml hygromycin B (Invitrogen). A human cervical epithelial cell line, HeLa [12], was transfected with rhesus macaque *CD1C* in pcDNA3.1(+) by a calcium phosphate precipitation method, and selection was performed as described above. These stably transfected cells were used as Ag-presenting cells (APCs) in T cell transfectants stimulation assays.

Flow cytometry. The expression of CD1 proteins on the surface of the LLC-MK2 cell transfectants as well as rhesus macaque thymocytes were analyzed by flow cytometry as described [13,14], using the BD FACSCanto II flow cytometer. The mouse monoclonal Abs (mAbs) used were 10H3 (anti-human CD1a) [15], SN13 (anti-human CD1b) (Ancell, Bayport, MN), M241 (anti-human CD1c) (Ancell), and SP34 (anti-monkey CD3) (BD Biosciences, Franklin Lakes, NJ). MAbs MOPC-31C (BD Biosciences) and RPC5.4 (ATCC) were used as negative controls.

T cell transfectants stimulation assays. TCR-deficient Jurkat cells, J.RT3, reconstituted with either the dideoxymycobactin-specific, CD1a-restricted TCR (J.RT3/CD8-2), the glucose monomycolate (GMM)-specific, CD1b-restricted TCR (J.RT3/LDN5) or the mannosyl phosphomycoketide-specific, CD1c-restricted TCR (J.RT3/CD8-1) have been described previously [16]. The TCR-reconstituted cells (5×10^4/well) were cultured with irradiated APCs expressing a relevant CD1 isoform (1×10^5/well) in wells of 96-well, flat-bottomed microtiter plates (200 μl media/well) in the presence of 10 ng/ml phorbol myristate acetate (PMA) (Sigma, St. Louis, MO) and either the organic extract of *Mycobacterium tuberculosis* H37Ra (for J.RT3/CD8-2 and J.RT3/CD8-1) or *Rhodococcus equi* GMM (for J.RT3/LDN5) at indicated concentrations. After 20 h, aliquots of the culture supernatants were collected, and the amount of interleukin-2 (IL-2) released into the supernatants was measured by the IL-2 ELISA kit (BD Biosciences).

Molecular modeling of rhesus macaque CD1b proteins. Molecular modeling of the rhesus macaque CD1b molecule was performed, using the homology modeling software PDFAMS (Protein Discovery Full Automatic Modeling System; In-Silico Sciences, Inc., Tokyo, Japan) as described [17]. Briefly, the primary sequence of the rhesus macaque CD1b molecule was aligned with the sequence of the human CD1b molecule available from the Protein Data Bank (1UQS), using RPS-BLAST. Amino acid residues differing between the two molecules were mutated, and the obtained 3-dimensional structure was optimized by the simulated annealing method. Subsequently, the molecular model was subjected to energy minimization, using the SYBYL software. The overall structure and the cavity surface of the modeled rhesus macaque CD1b molecule were depicted in association with GMM from *Nocardia farcinica* by utilizing the MOLCAD module of SYBYL.

Results and discussion

Identification of rhesus macaque group 1 CD1 cDNAs

To isolate full-length cDNAs encoding rhesus macaque CD1a and CD1b, the first strand cDNA was synthesized from lymph node total RNA by reverse transcription, and then, PCR was carried out with specific pairs of 5′-end and 3′-end primers that were designed based on the rhesus macaque genomic *CD1A* and *CD1B* sequences. The rhesus macaque genomic *CD1C* sequence was only partially available, and the 3′-end sequence was undermined. Therefore, rhesus macaque *CD1C* cDNA was amplified by PCR using a specific 5′-end primer and a 3′-end primer that was designed based on the sequence of 3′-untranslated region of the human *CD1C* genome. The PCR products thus obtained were of expected size (approximately 1 kb) and the identity of the products was determined by DNA sequences. Identical nucleotide sequences were obtained after two independent PCR amplifications, ruling out the possibility for PCR-associated errors.

Alignment of the deduced amino acid sequences of the putative rhesus macaque *CD1A*, *CD1B*, and *CD1C* genes with the corresponding human CD1 proteins revealed a high-degree homology between the two species (85.6% for CD1a, 94.6% for CD1b, 90.4% for CD1c) (Fig. 1). The cysteine residues (indicated with triangles) involved in the intrachain disulfide bond formation in the α2 and the α3 domains as well as the putative N-linked glycosylation sites (indicated with asterisks) in the α1 and the α2 domains were totally conserved [2]. Further, the cytoplasmic tyrosine-based motif (YXXZ where Y is tyrosine, X is any amino acid, and Z is a hydrophobic amino acid) and its flanking sequences that are known to regulate differential early endosomal and lysosomal trafficking of CD1b and CD1c proteins [12,18,19] were identical between the two species (Fig. 1).

To monitor protein expression of these rhesus macaque *CD1* genes, we first screened mAbs against human CD1 proteins for their cross-reactivity to rhesus macaque thymocytes, a cell type that is presumed to express all forms of group 1 CD1 molecules. As shown in Fig. 2A, mAb clones 10H3 (anti-human CD1a), SN13 (anti-human CD1b), and M241 (anti-human CD1c) labeled a significant fraction of $CD3^{dim}$ thymocytes in a pattern comparable to that for human thymocytes [20]. We then stably transfected each

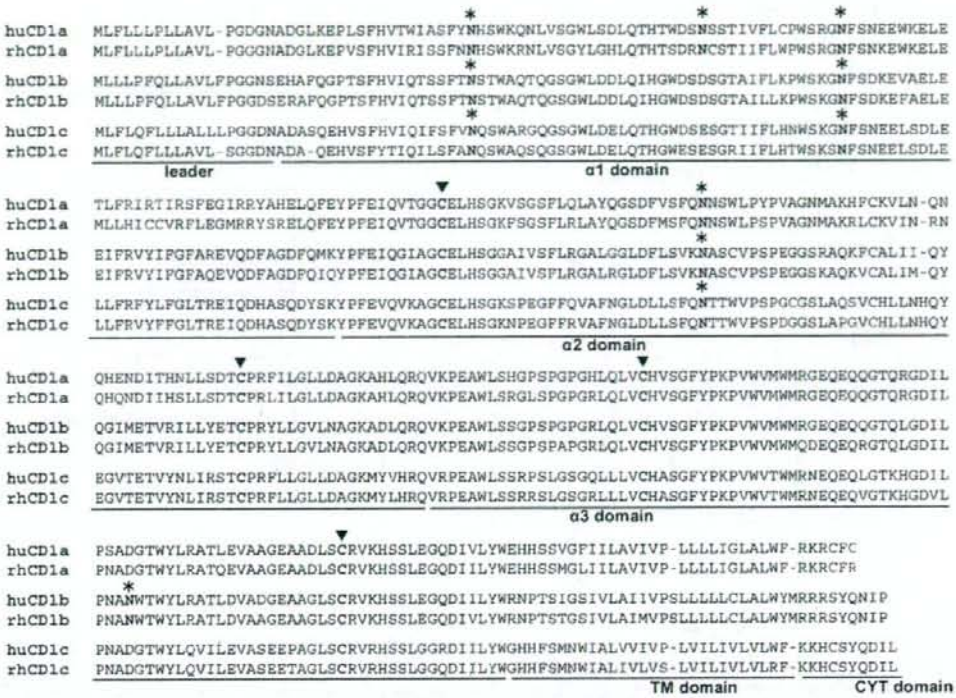

Fig. 1. Alignment of deduced amino acid sequences of human (hu) and rhesus macaque (rh) group 1 CD1 proteins. Residues conserved between the two species are shaded in light gray. Solid triangles denote cysteines conserved in all the group 1 CD1 proteins of both species that are presumed to be involved in intradomain disulfide bond formation. Asterisks indicate potential N-linked glycosylation sites. Dashes represent gaps that have been introduced to maximize alignment. TM domain, transmembrane domain; CYT domain, cytoplasmic domain.

of the putative rhesus macaque *CD1A*, *CD1B*, and *CD1C* genes into a rhesus macaque kidney epithelial cell line, LLC-MK2, and their protein expression was monitored by flow cytometry using the cross-reactive mAbs (Fig. 2B). The 10H3 anti-human CD1a mAb recognized only *CD1A* transfected cells, but not those transfected with the other genes. Similarly, the SN13 anti-human CD1b mAb and the M241 anti-human CD1c mAb showed specific reactivity to cells transfected with the *CD1B* and the *CD1C* genes, respectively. These results provided both evidence for protein expression of the isolated genes and further support for their identity, and therefore, the nucleotide sequences of the putative *CD1A*, *CD1B*, and *CD1C* cDNAs were deposited to the DDBJ/GenBank/EMBL databases as those of rhesus macaque *CD1A* (Accession Nos: AB458511), *CD1B* (AB458512), and *CD1C* (AB458513), respectively.

Trans-species activation of human T cells by rhesus macaque CD1b molecules

With the exception of mice and rats, group 1 CD1 genes have been identified in virtually all mammalian animals so far analyzed, but the Ag presentation function of their products has not been demonstrated so explicitly as in humans [21]. This is partly due to difficulties in obtaining specific T cell lines and clones that recognize lipid Ags in the context of CD1 molecules of a given animal species. Because of the highly conserved amino acid sequences of human and rhesus macaque group 1 CD1 proteins, we considered the possibility that rhesus macaque CD1 molecules might bind lipid Ags that were known to be presented by human CD1 molecules, and interact with specific human TCRs. To address this, human TCRs derived either from a dideoxymycobactin-specific, CD1a-restricted T cell line (CD8-2), from a GMM-specific, CD1b-restricted T cell line (LDN5) or from a mannosyl phosphomycoketide-specific, CD1c-restricted T cell line (CD8-1) were reconstituted in TCR-deficient Jurkat cells (J.RT3) by gene transfer, and the T cell reactivity to specific Ag in the presence of cell transfectants expressing a relevant CD1 isoform of either human or rhesus macaque origin was assessed by measuring IL-2 released from the T cells. J.RT3/CD8-2 cells responded to dideoxymycobactin in the presence of APCs expressing human CD1a molecules, but not those expressing rhesus macaque CD1a molecules (Fig. 3, top panel). Similarly, J.RT3/CD8-1 cells responded to mannosyl phosphomycoketide in the presence of APCs expressing human CD1c molecules, but not those expressing rhesus macaque CD1c molecules (bottom panel). Strikingly, however, APCs expressing rhesus macaque CD1b molecules were capable of presenting GMM efficiently to J.RT3/LDN5 cells (middle panel), providing evidence for their Ag presentation function. The apparently more efficient Ag presentation function for rhesus macaque CD1b molecules as compared with human CD1b molecules could be accounted for by the slightly higher expression on rhesus macaque CD1b transfectants than on human CD1b transfectants (data not shown).

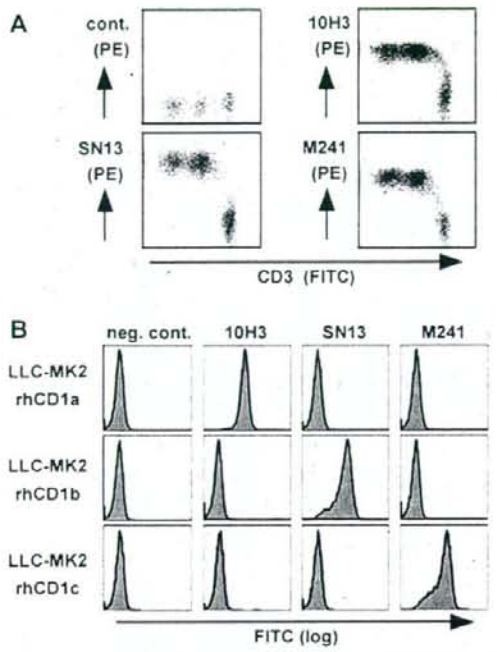

Fig. 2. Cross-reactivity of anti-human CD1 mAbs to rhesus macaque group 1 CD1 proteins. (A) Rhesus macaque thymocytes were double-labeled with the SP34 anti-CD3 mAb and either the 10H3 anti-human CD1a mAb, the SN13 anti-human CD1b mAb, the M241 anti-human CD1c mAb, or negative control Abs, followed by analysis by flow cytometry. (B) A rhesus macaque kidney cell line, LLC-MK2, that stably transfected with either rhesus macaque *CD1A* (LLC-MK2 rhCD1a), *CD1B* (LLC-MK2 rhCD1b), or *CD1C* (LLC-MK2 rhCD1c) were labeled with indicated mAbs and analyzed by flow cytometry.

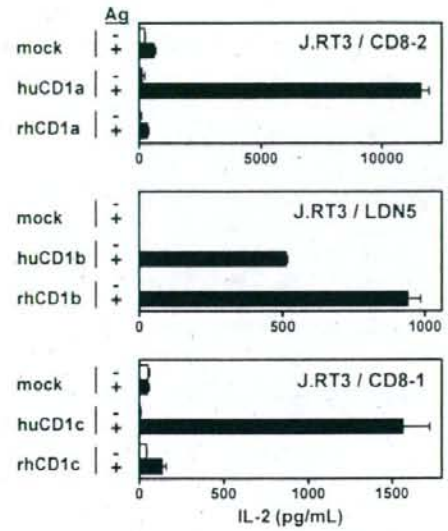

Fig. 3. Ag presentation function of rhesus macaque CD1b molecules. The J.RT3/CD8-2 cells were cultured in the presence or absence of the organic extract of *M. tuberculosis* (50 mg/ml) with T2 cells expressing either human CD1a (huCD1a) or rhesus macaque CD1a (rhCD1a) or those that were mock-transfected (top panel). The J.RT3/LDN5 cells were cultured in the presence or absence of purified GMM (5 mg/ml) with T2 cells expressing either human CD1b (huCD1b) or rhesus macaque CD1b (rhCD1b) or those that were mock transfected (middle panel). The J.RT3/CD8-1 cells were cultured in the presence or absence of the organic extract of *M. tuberculosis* (1.56 mg/ml) with HeLa cells expressing either human CD1c (huCD1c) or rhesus macaque CD1c (rhCD1c) or those that were mock transfected (bottom panel). After 20 h, the culture supernatants were harvested and the amount of IL-2 secreted into the supernatants were measured.

Trans-species crossreaction has never been observed previously for any of the group 1 CD1 molecules. Nevertheless, a molecular model of the rhesus macaque CD1b molecule has detected the α1 and α2 helix structure as well as intramolecular pockets (A′, C′, and F′) and a tunnel (T′) virtually identical to those for human CD1b molecules [22,23], allowing stable interaction with a human CD1b-presented mycobacterial Ag, GMM (Fig. 4). Further, amino acid residues, such as E80 and D83 in the α1 domain and T157 and T165 in the α2 domain, that are proposed to be critical for interaction with specific TCRs [24] are shared between rhesus macaque and human CD1b molecules, suggesting a conserved function for CD1b in these two species. The extent of amino acid sequence conservation is higher in CD1b than in CD1a and CD1c (Fig. 1), which may imply that immune responses to mycolic acid-containing glycolipds are critical for host defense against tuberculosis. So far, no experimental animals have proved extremely useful as a model for studying the group 1 CD1-mediated immunity in human infectious diseases. The present study underscores that monkeys are indispensable for a variety of challenges, including development of a new type of lipid-based vaccines against tuberculosis.

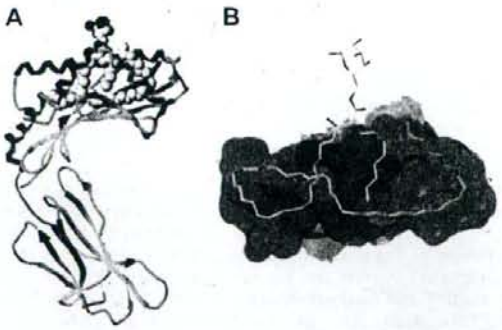

Fig. 4. A molecular model of rhesus macaque CD1b proteins. The rhesus macaque CD1b structure was constructed, based on the crystal structure of the human CD1b-GMM complex. (A) The overall structure of the rhesus macaque CD1b-GMM complex is shown, in which the CD1b heavy chain is depicted in ribbon diagram and the non-hydrogen atoms of GMM are drawn as van der Waals spheres (carbon in gray; oxygen in red). The associated β2-microglobulin is not depicted for simplicity purposes. (B) The binding surface of the Ag-binding groove is drawn in green with the bound GMM in stick (carbon in gray; oxygen in red). (For interpretation of the references to colour in this figure legend, the reader is referred to the web version of this paper).

Acknowledgments

We thank Drs. M. Brenner, D. Olive, and C. Mawas for their gifts of reagents. This work was supported by grants from the Ministry of Education, Culture, Sports, Science and Technology (Grant-in-Aid from Scientific Research on Priority Areas), from the Japan Society for the Promotion of Science (Grant-in-Aid for Scientific Research

(B)), and from the Ministry of Health, Labour, and Welfare (Research on Emerging and Re-emerging infectious Diseases) (to M.S.).

References

[1] C.T. Morita, R.A. Mariuzza, M.B. Brenner, Antigen recognition by human gamma delta T cells: pattern recognition by the adaptive immune system, Springer Semin. Immunopathol. 22 (2000) 191–217.
[2] S.A. Porcelli, The CD1 family: a third lineage of antigen-presenting molecules, Adv. Immunol. 59 (1995) 1–98.
[3] R.J. North, Y.J. Jung, Immunity to tuberculosis, Annu. Rev. Immunol. 22 (2004) 599–623.
[4] T. Mogues, M.E. Goodrich, L. Ryan, R. LaCourse, R.J. North, The relative importance of T cell subsets in immunity and immunopathology of airborne *Mycobacterium tuberculosis* infection in mice, J. Exp. Med. 193 (2001) 271–280.
[5] C.C. Dascher, K. Hiromatsu, J.W. Naylor, P.P. Brauer, K.A. Brown, J.R. Storey, S.M. Behar, E.S. Kawasaki, S.A. Porcelli, M.B. Brenner, K.P. LeClair, Conservation of a CD1 multigene family in the guinea pig, J. Immunol. 163 (1999) 5478–5488.
[6] K. Hiromatsu, C.C. Dascher, M. Sugita, C. Gingrich-Baker, S.M. Behar, K.P. LeClair, M.B. Brenner, S.A. Porcelli, Characterization of guinea-pig group 1 CD1 proteins, Immunology 106 (2002) 159–172.
[7] D.H. Barouch, J. Kunstman, M.J. Kuroda, J.E. Schmitz, S. Santra, F.W. Peyerl, G.R. Krivulka, K. Beaudry, M.A. Lifton, D.A. Gorgone, D.C. Montefiori, M.G. Lewis, S.M. Wolinsky, N.L. Letvin, Eventual AIDS vaccine failure in a rhesus monkey by viral escape from cytotoxic T lymphocytes, Nature 415 (2002) 335–339.
[8] Y. Shen, D. Zhou, L. Qiu, X. Lai, M. Simon, L. Shen, Z. Kou, Q. Wang, L. Jiang, J. Estep, R. Hunt, M. Clagett, P.K. Sehgal, Y. Li, X. Zeng, C.T. Morita, M.B. Brenner, N.L. Letvin, Z.W. Chen, Adaptive immune response of Vgamma2Vdelta2+ T cells during mycobacterial infections, Science 295 (2002) 2255–2258.
[9] R.N. Hull, W.R. Cherry, O.J. Tritch, Growth characteristics of monkey kidney cell strains LLC-MK1, LLC-MK2, and LLC-MK2(NCTC-3196) and their utility in virus research, J. Exp. Med. 115 (1962) 903–918.
[10] M.L. Wei, P. Cresswell, HLA-A2 molecules in an antigen-processing mutant cell contain signal sequence-derived peptides, Nature 356 (1992) 443–446.
[11] M. Sugita, E.P. Grant, E. van Donselaar, V.W. Hsu, R.A. Rogers, P.J. Peters, M.B. Brenner, Separate pathways for antigen presentation by CD1 molecules, Immunity 11 (1999) 743–752.
[12] M. Sugita, X. Cao, G.F. Watts, R.A. Rogers, J.S. Bonifacino, M.B. Brenner, Failure of trafficking and antigen presentation by CD1 in AP-3-deficient cells, Immunity 16 (2002) 697–706.
[13] M. Cernadas, M. Sugita, N. van der Wel, X. Cao, J.E. Gumperz, S. Maltsev, G.S. Besra, S.M. Behar, P.J. Peters, M.B. Brenner, Lysosomal localization of murine CD1d mediated by AP-3 is necessary for NK T cell development, J. Immunol. 171 (2003) 4149–4155.
[14] H. Suzuki, M. Motohara, A. Miyake, K. Ibuki, Y. Fukazawa, K. Inaba, K. Masuda, N. Minato, H. Kawamoto, M. Hayami, T. Miura, Intrathymic effect of acute pathogenic SHIV infection on T-lineage cells in newborn macaques, Microbiol. Immunol. 49 (2005) 667–679.
[15] D. Olive, P. Dubreuil, C. Mawas, Two distinct TL-like molecular subsets defined by monoclonal antibodies on the surface of human thymocytes with different expression on leukemia lines, Immunogenetics 20 (1984) 253–264.
[16] E.P. Grant, M. Degano, J.P. Rosat, S. Stenger, R.L. Modlin, I.A. Wilson, S.A. Porcelli, M.B. Brenner, Molecular recognition of lipid antigens by T cell receptors, J. Exp. Med. 189 (1999) 195–205.
[17] C.E. Wheelock, Y. Nakagawa, T. Harada, N. Oikawa, M. Akamatsu, G. Smagghe, D. Stefanou, K. Iatrou, L. Swevers, High-throughput screening of ecdysone agonists using a reporter gene assay followed by 3-D QSAR analysis of the molting hormonal activity, Bioorg. Med. Chem. 14 (2006) 1143–1159.
[18] M. Sugita, R.M. Jackman, E. van Donselaar, S.M. Behar, R.A. Rogers, P.J. Peters, M.B. Brenner, S.A. Porcelli, Cytoplasmic tail-dependent localization of CD1b antigen-presenting molecules to MIICs, Science 273 (1996) 349–352.
[19] M. Sugita, N. Van Der Wel, R.A. Rogers, P.J. Peters, M.B. Brenner, CD1c molecules broadly survey the endocytic system, Proc. Natl. Acad. Sci. USA 97 (2000) 8445–8450.
[20] L.L. Lanier, J.P. Allison, J.H. Phillips, Correlation of cell surface antigen expression on human thymocytes by multi-color flow cytometric analysis: implications for differentiation, J. Immunol. 137 (1986) 2501–2507.
[21] K. Hiromatsu, C.C. Dascher, K.P. LeClair, M. Sugita, S.T. Furlong, M.B. Brenner, S.A. Porcelli, Induction of CD1-restricted immune responses in guinea pigs by immunization with mycobacterial lipid antigens, J. Immunol. 169 (2002) 330–339.
[22] T. Batuwangala, D. Shepherd, S.D. Gadola, K.J. Gibson, N.R. Zaccai, A.R. Fersht, G.S. Besra, V. Cerundolo, E.Y. Jones, The crystal structure of human CD1b with a bound bacterial glycolipid, J. Immunol. 172 (2004) 2382–2388.
[23] S.D. Gadola, N.R. Zaccai, K. Harlos, D. Shepherd, J.C. Castro-Palomino, G. Ritter, R.R. Schmidt, E.Y. Jones, V. Cerundolo, Structure of human CD1b with bound ligands at 2.3 A, a maze for alkyl chains, Nat. Immunol. 3 (2002) 721–726.
[24] A. Melian, G.F. Watts, A. Shamshiev, G. De Libero, A. Clatworthy, M. Vincent, M.B. Brenner, S. Behar, K. Niazi, R.L. Modlin, S. Almo, D. Ostrov, S.G. Nathenson, S.A. Porcelli, Molecular recognition of human CD1b antigen complexes: evidence for a common pattern of interaction with alpha beta TCRs, J. Immunol. 165 (2000) 4494–4504.